Using sonar habitat mapping and GIS analyses to identify freshwater mussel habitat and estimate population size of a federally endangered freshwater mussel species, *Amblema neislerii*, in the Apalachicola River, FL

by

Reuben B. Smit

A thesis submitted to the Graduate Faculty of
Auburn University
in partial fulfillment of the
requirements for the Degree of
Master of Science

Auburn, Alabama
May 3, 2014

Keywords: sonar habitat mapping, freshwater mussels, species distribution model, *Amblema neislerii*, fat threeridge, Apalachicola River

Approved by

James Stoeckel, Chair, Associate Professor, School of Fisheries, Aquaculture, and Aquatic Sciences
Elise R. Irwin, Associate Professor, School of Fisheries, Aquaculture, and Aquatic Sciences
Steven M. Sammons, Research Fellow IV, School of Fisheries, Aquaculture, and Aquatic Sciences
Adam J. Kaeser, United States Fish and Wildlife Service
Michael Gangloff, Assistant Professor, Department of Biology, Appalachian State University

Abstract

Identification and quantification of freshwater mussel habitat in large turbid rivers is challenging. Sonar habitat mapping offers a low cost and time efficient means to identify and quantify benthic habitats over large spatial extents. I used sonar to classify freshwater mussel habitat across a 700 hectare reach of the Apalachicola River, FL, and used sonar imagery collected before and after a 10-year flood event to assess habitat stability. GIS-derived metrics and survey data were used to develop predictive models of presence/absence and abundance for the federally endangered freshwater mussel, *Amblema neislerii*. Strong associations were identified between habitats representing flow refugia, as well as deep water habitats. I validated predicted abundances with data from an independent, quantitative study. Suitable *A. neislerii* habitat as revealed by this approach was much larger than identified in previous studies, as was the resulting reach-wide population estimates of 7-8 million individuals.

Acknowledgements

I must thank many people of highest quality that made this manuscript possible, and those who contributed greatly to the lessons learned during the process. Each of my committee members collaborated a great deal and greatly improved my understanding of the scientific discipline and writing. Adam Kaeser has taught me everything I know about sonar habitat mapping, and his creativity, enthusiasm, and critical thinking made this project successful. Mike Gangloff sampled technically challenging habitats for the ground-breaking benefit of this study, and contributed greatly to this study through provision of data and encouragement. Jim Stoeckel provided patient guidance through the complicated world of academia. Steve Sammons and Elise Irwin gave essential comments that improved my writing significantly. I would like to give a shout-out to my Auburn University labmates Michael Hart, Tyler Mosely, and Ian Palmer for help with fieldwork, as well as for many intelligent discussions and welcomed diversions that made my experience in Auburn meaningful. Also, the USFWS crew in Panama City, Florida deserves recognition for outstanding field assistance, support, and friendship.

Table of Contents

List of Tables

List of Figures

I. Using side scan sonar to delineate freshwater mussel habitat and assess habitat stability in a meandering Coastal Plain river.

Introduction

Classifying and quantifying freshwater mussel habitat in large rivers is challenging. Large rivers impose a variety of logistical hurdles when attempting to access and measure physical or biological components of the benthic environment. The investigation of habitat associations over large spatial extents requires that practitioners strive to balance feasibility and effectiveness when conducting research and conservation activities.

Freshwater mussel habitat has been broadly linked to landscape-scale factors such as land-use, catchment size, and stream power (DiMaio & Corkum 1995; Arbuckle & Downing 2001; McRae 2004), and to micro-habitat characteristics such as substrate type, particle size, food availability, and the presence of fish hosts (Brainwood et al. 2008; Hastie et al. 2000; Brim Box et al. 2002; Vaughn & Taylor 2000). Micro-scale measurements of depth, particle size, and current velocity used in complex hydraulic modeling and assessments of sediment stability have provided compelling evidence that mussel beds occur in areas where substrate remains stable during base flow and high-discharge events (Morales et al. 2006; Steuer et al. 2008; Zigler et al. 2008; Allen & Vaughn 2010).

Identifying how ecological processes function across spatial scales is becoming a key area in ecological research (Levin 1992), and clearly identifying the spatial scale and associated factors in which the phenomenon of interest is occurring is essential for any study of freshwater mussel ecology (Newton et al. 2008). Fausch et al. (2002) identified the importance of intermediate-scale processes to the ecology of stream fishes, and noted that they provide

important ecological details that may be overlooked when only micro and landscape scales are considered. Intermediate (meso-scale) habitat classifications have been shown to be practical and effective when applied to biological habitat assessments across wide geographic boundaries (Newson and Newson 2000). With the preponderance of freshwater mussel habitat studies occurring at the landscape and micro scales, the science of freshwater mussel ecology might be advanced by studies conducted at the meso-scale.

Micro-scale assessments of substrate stability can be used to calibrate meso-scale models that predict hydraulically stable habitats across larger spatial extents than is feasible with micro-scale studies alone (Parasiewicz et al. 2012). Although metrics such as relative substrate stability are assessed at a fine scale through integration of particle size and shear velocity measurements, hydraulically stable habitats often occur and can be identified as patches at a higher spatial scale (Morales et al. 2006). Patch units are commonly used in landscape ecology as classes of predominant habitat within a spatial context, and occur at intermediate spatial scales (Newson and Newson 2000). Areas of hydraulic refuge in streams represent patches of suitable habitat for many organisms, increasing the richness, diversity, and abundance of aquatic species (Townsend et al. 1989; Garcia et al. 2012), including freshwater mussels (Strayer et al. 1999). Thus, incorporating meso-scale information such as patch-level habitat data in studies may advance understanding of freshwater mussel ecology in large rivers.

The close relationship between the hydraulic habitat needs of freshwater mussels and the spatial extent at which these habitat units exist suggests that study of freshwater mussel habitat at the meso-scale and patch level may provide useful information for the conservation of these imperiled benthic animals. However, measurement and derivation of complex hydraulic components to predict substrate stability requires expensive equipment and significant time,

effort, and expertise, which may limit the widespread adoption of this approach. Although complex hydraulic variables are clearly useful and important to identify stable habitat for freshwater mussels, aquatic resource managers could benefit from low-cost tools and approaches to identify and accurately quantify suitable, stable mussel habitat within the logistical constraints imposed by time, money, and scale.

Remote sensing of benthic features using side scan sonar provides detailed information on benthic habitat in hard to access environments. Sonar habitat mapping and geographic information system (GIS) techniques can be integrated to classify and quantify benthic habitats in large rivers (Strayer et al. 2006; Nitsche et al. 2007), and riverine habitat features such as woody material and substrates have been accurately mapped using relatively low cost sonar equipment (Kaeser & Litts 2008; 2010; Kaeser et al. 2012). Sonar imaging techniques have been used to track sedimentation processes and bedform in riverine environments (Amina et al. 2007; Nitsche et al. 2007; Manley and Singer 2007). Bedforms that represent turbulent, unstable hydraulic conditions might therefore be discriminated from those associated with more stable conditions by sonar imaging.

Large meandering rivers are shaped by sediment transport forces and exhibit hydraulic patterns that support the formation of stable habitat patches in predictable locations across the river channel (Klienhans et al. 2010; Garcia et al. 2012). In alluvial rivers, variability in hydraulic forces due to meandering flow dramatically influence the shape and conditions of the river channel, and support the formation of large sand dunes that migrate downstream during action stages of river flows (Deitrich et al. 1979). In sonar imagery, dune bedform features can be easily recognized (Elliot et al. 2004), and are associated with the high shear stresses regions of the channel (Arcement and Schnieder 1989; Zigler et al. 2008; Garcia et al. 2012). As large

rivers change direction around a meander bend, the scouring erosional forces of river flows separate from the bank and create secondary backwater/eddy flow environments and recirculation zones, that occur both upstream and downstream of point bars and adjacent to the river bank (Ferguson et al. 2003). These areas are used as hydraulic refuge by benthic organisms including freshwater mussels during flood disturbances (Strayer 1999; Morales 2006; Steuer et al. 2008; Zigler et al. 2008; Garcia et al. 2012). Flow refugia are also used by a variety of fish species that may serve as hosts for mussels, thereby increasing chances of glochidial deposition in these areas.

The Apalachicola River in northwest Florida is a large, alluvial river that is home to a variety of endemic species, including several imperiled freshwater mussels (Brim Box and Williams 2000). The fat threeridge, *Amblema neislerii*, is a federally endangered species, and is most abundant in the middle reach of the Apalachicola as well as the lower Chipola River, an adjacent tributary (Gangloff 2012). Quantification of *A. neislerii* habitat throughout the Apalachicola River was identified as a high priority by the U.S. Fish and Wildlife Service (USFWS) for conservation and recovery of the species (USFWS Recovery Plan 2010). A map of potential mussel habitat is needed to stratify mussel sampling, and to provide data for modeling the distribution and abundance of *A. neislerii* throughout the river.

Preliminary sonar imaging of known mussel beds in the Apalachicola River revealed distinct, observable differences in characteristics of the sandy bottom (A. Kaeser 2012, unpublished data). In particular, a smooth bedform was observed in locations of known mussel beds. This flat, plane bedform extended some distance away from the bank of the river and ended abruptly at a boundary of distinctive sand dune and ripple bedforms. Smooth bedforms were found both upstream and downstream of sandy point bars throughout a meandering reach of the

Apalachicola River known to support a high diversity and abundance of freshwater mussels, including *A. neislerii* (Brim Box & Williams 2000). Variations in bedform observed in the sonar imagery were interpreted as indicators of the hydraulic conditions at the water/sediment interface during the bed-forming, action stages of river discharge, and were further suspected to correspond to differences in habitat suitability for mussels. Bedform topology has been used for meso-scale habitat classification (Frissel et al. 1986), and the hydraulic conditions of meander bends are responsible for the spatial arrangement of bedforms within the channel, further suggesting the phenomena of interest could be described well at the meso-scale of study (Newson & Newson 2000; Garcia et al. 2012). I hypothesized that low-cost, sonar habitat mapping would enable the classification of suitable mussel habitat at the meso-scale.

My first goal was to identify and implement a classification scheme for benthic mesohabitat units that would represent functional habitat for freshwater mussels in a large, coastal plain river. In order to assess temporal consistency of mesohabitat boundaries, I also used sonar imagery to quantify the areal change that occurred to the mesohabitat classes after a 10-year flood event. Thus, my objectives were to: (1) validate the use of low-cost, sonar habitat mapping for classifying and quantifying area of mesoscale habitat patches based on bedform features, and (2) assess the stability of mesohabitat units suspected to function as flow refugia for mussels using pre and post-flood sonar imaging and areal change analysis within a GIS platform.

Methods

Study Area

The Apalachicola River is a large alluvial river formed at the confluence of the Chattahoochee River and the Flint River, and since impoundment begins below Jim Woodruff

Lock and Dam, a navigation and hydropower facility, at the Georgia/Florida state boundaries (Figure 1). The Apalachicola River drains 50,800 km^2 of eastern Alabama, west and central Georgia, and portions of northwestern Florida making it the largest river in Florida and ranking it 21st in mean annual discharge in the United States (Light et al. 1998). The Apalachicola River is currently regulated to maintain a minimum flow of 141.5 m^3s^{-1} (5,000 f^3s^{-1}) during low flow periods of the year (USFWS 2012).

Below the Jim Woodruff Lock and Dam the Apalachicola River flows unimpeded for 174 km to the Gulf of Mexico. Along its course trends in channel morphology allow division of the river into Upper, Middle, and Lower-Non Tidal reaches (Light et al. 2006). The Upper section exhibits a relatively straight channel composed of coarse sand and gravel with scattered limestone outcroppings that continues until river kilometer (rkm) 130, the point at which the surrounding geology drops from the Tallahassee Hills to the Coastal Lowlands (Harvey 2007). At this point channel geomorphology begins to exhibit a strong meandering characteristic and sediment composition changes to primarily coarse and fine sand. At rkm 67, the main channel exhibits a natural anabranch diversion known as the Chipola cut-off, which connects the Apalachicola River to the Chipola River, a large tributary. The Chipola cut-off marks the end of the Middle Reach and the beginning of the Lower-Non Tidal Reach. The Lower-Non Tidal Reach exhibits repeating meander bends until rkm 57. Thereafter the river assumes a less sinuous course, and continues toward Apalachicola Bay, whose tidal influences from the Gulf of Mexico begin to influence the shape and chemistry of the channel.

In this study, I focused on the Middle Reach and an upstream portion of the Lower Non-Tidal Reach of the Apalachicola River (rkm 104-54; river mile (RM) 65-35; Figure 1), because these portions are known to hold the highest abundance and diversity of freshwater mussels and

a majority of the Apalachicola River population of *A. neislerii* (Brim Box & Williams 2000; Gangloff 2012).

Sonar Survey and Image Processing

Sonar imagery of the entire study area was collected using a Humminbird® 1198c side-imaging sonar unit during the first two weeks of March 2012 (3/2, 3/7, 3/15, and 3/16) and a 17-foot skiff equipped with a custom, front-mounted sonar transducer (Kaeser and Litts 2011). River flows of 566 m^3s^{-1} (15,000 f^3s^{-1}) or greater were targeted for the survey, as the river channel is fully inundated at these discharges (Figure 2). The middle reach of the river often exceeded 100 m in width at the target flows, thus, a 3-pass, multi-transect approach was required to maintain high image resolution across the entire channel. One survey pass (i.e., transect) was made within close proximity of each bank of the river, using a sonar range setting of 26 m per side. A third pass was made along the middle of the river channel using a sonar range setting of 45.7 m per side to image the gap between the two bankside transects. I opted to use a lower range setting during bank passes to provide higher image resolution in areas known to harbor mussel beds. Slant range correction, an option referred to as "water contour mode" in the Humminbird® side imaging system, was not activated during bank passes. Slant range correction is a processing feature that removes the water column representation from sonar images, but I determined this feature performed poorly when imaging areas containing large quantities of submerged wood. Slant range correction was enabled, however, during scanning of the middle transect because it was largely devoid of wood. An operating frequency of 455 kHz was used during all sonar survey passes. In addition to sonar imagery, depth observations were recorded at 3-second intervals along all survey routes.

Sonar image geoprocessing was conducted according to methods described in Kaeser and Litts (2011). Once processed, the sonar image maps (SIMs, i.e., rectified image raster datasets) were loaded into an ESRI ArcGIS workspace to provide a spatially continuous, 2-dimensional representation of the river bottom across the entire study area.

Habitat Mapping

A mesohabitat classification scheme was developed through a review of literature associated with large river habitat classifications and discussions with biologists familiar with the Apalachicola River and with mussel sampling in the system. Five distinct habitat classes were identified as occurring within the main river channel: Point Bar, Inner Recirculation Zone, Outer Recirculation Zone, Mid-Channel, and Pool/Outer Bank. Garcia et al. (2012) provided technical explanations of the hydrological conditions likely to be occurring within each of these mesohabitat classes. Mesohabitat classes and their associated definitions are summarized in Table 1, and a visual representation of the geospatial context and general hydraulic conditions of each class within a meander bend is portrayed in Figure 3.

Mesohabitat classes were delineated using a heads-up, manual digitization approach during inspection of the sonar image map (SIM) layers (Kaeser and Litts 2011). River banks were first digitized as an outer boundary for the mesohabitat class delineation. Banks were kept within view on-screen during near-bank survey passes and were digitized as the apparent boundary of the sonar signal reflectance. Following bank digitization, boundaries between bank-attached, plane (i.e., smooth) bedforms and rippled/dune patterns were drawn.

Since slant range correction was not applied during near-bank passes, a standardized approach to digitizing features that appeared near to, and/or crossing the dark band of pixels

representing the water column in the middle of resulting images was necessary. Whenever the water column is incorporated in a sonar image, objects or features that exist directly beneath the boat during the survey are both compressed and displaced to either side of the water column to some extent. As such, the water column does not represent missing data, but its inclusion does introduce some positional error and feature distortion. My approach to digitizing boundary features in such imagery was to trace the boundary as it appeared in the SIMs until the boundary intersected the water column pixels. At this point, the actual boundary was located directly beneath the survey vessel, so I digitized the boundary as a line that crossed the water column and followed the center of the image until the boundary feature was again visible on the opposite side of the water column. When visible, the boundary would be drawn across the water column and proceeding along the apparent position of the feature in the SIMs (Figure 4). This approach provided a consistent and repeatable method for digitizing features when the water column was displayed, but may have introduced some positional error associated with features that occurred near the boat path.

After the bank-attached, smooth bedform regions of the channel were separated from the rippled and duned channel regions, the Inner and Outer Recirculation Zones were dissected from the Pool/ Outer Bank. Since three mesohabitats exhibited smooth bedform in the SIMs, alternate features were used for this delineation. The downstream extent of the Inner Recirculation Zone was generally recognizable in the SIMs by the appearance of large pieces of submerged wood, a change in substrate tone from dark to light, and a change in the appearance of the bank edge from a dull-toned, less discrete edge to a bright, solid edge indicating a steepening of the bank slope (Figure 5). The Outer Recirculation Zone was delineated from the Pool/Outer Bend with similar sonar features as the Inner Recirculation Zone. At this transition, a darkening of image

tone was often apparent, likely due to the deposition of finer particles (i.e., silt and mud). Also apparent at this transition was a change in the bank signature from bright and narrow to fuzzy and broad, indicating a reduction of the bank slope (Figure 5). The quantity of large woody material appeared to be similarly abundant in both mesohabitats and was not a useful characteristic for discriminating the Pool/Outer Bank from the Outer Recirculation Zone. To interpret the transition between the Pool/Outer Bank and the Outer Recirculation Zone, I also identified an inflection point at which the depth of water along the Pool/Outer Bank began to decrease, indicating the beginning of the pool tail-out and a change in the flow environment along the river margin.

Delineation of the Point Bar from the Mid-Channel required incorporation of aerial imagery and knowledge of deposition patterns around meander bends. At action stages, when the bed is formed, the point bar is submerged and shows no clear separation in terms of bedform from the Mid-Channel in sonar imagery. However, once flows recede seasonally the shallowest portions of point bars become exposed and can be clearly seen in aerial imagery. To delineate a portion of the point bar that remained inundated at seasonally low flow levels, a narrow (~10 m wide) portion of the Mid-Channel surrounding the exposed point bar was separated from the Mid-Channel using 2010 National Agricultural Inventory Program (NAIP) aerial imagery collected during a period of low flow (141.5 m^3s^{-1}/ 5,000 f^3s^{-1}). The resulting area of shallow, inundated river channel adjacent to point bars was classified as the Point Bar mesohabitat. The Point Bar mesohabitat was assigned a unique class on the basis that it might differ from the Mid-Channel mesohabitat class in terms of physical habitat conditions.

The Apalachicola River is currently regulated to maintain a minimum flow of 141.5 m^3s^{-1} (5,000 f^3s^{-1}) during low flow periods of the year (USFWS 2012). To identify the extent of habitat

inundated at this low flow level, and subsequently map only the habitat that is available to mussels during such conditions, I digitized the river bank and the edge of exposed sand bars using recent (Summer 2010) National Agricultural Inventory Program (NAIP) aerial imagery captured during a period of stable, low flow (141.5 m^3s^{-1}/5000 f^3s^{-1}). This boundary was incorporated in the habitat map and used to define the extent of habitat available to mussels during low flow conditions. Sloughs and other off-channel, inundated areas were not included in the habitat classification scheme and therefore were not mapped in this study.

In order to investigate habitat composition trends across the longitudinal extent of the study area, the final habitat map was decomposed into consecutive sites containing representatives of all mesohabitat classes. The boundaries of each site were delineated as lines drawn between the downstream ends of each pair of Inner and Outer Recirculation Zones occurring on adjacent sides of the river. Therefore, and with few exceptions, each site contained only one representative of each mesohabitat class. I extracted areal values for all mapped mesohabitats and summarized both the overall and relative composition of each site to illustrate trends in habitat composition. To investigate river gradient as a factor potentially associated with the geomorphology of these sites, I extracted water surface elevation values derived from a LIDAR-based survey along the river course at 0.16 km intervals. Water surface elevation was plotted against rkm to illustrate trends in water surface slope occurring throughout the study reach.

Assessing mesohabitat consistency between pre and post flood sonar imagery

Side scan sonar has been used to track changes in river bedforms after flood events (Anima et al. 2007). In March 2013 the Apalachicola River experienced a 10-year flood event

where discharge recorded at the USGS gauge in Chattahoochee, FL exceeded 2,832 m^3s^{-1} (100,000 f^3s^{-1}) (Figure 2). This flood followed a high discharge event where flow peaked above 2,265 m^3s^{-1} (80,000 f^3s^{-1}). Recognizing an opportunity to assess changes occurring to the areal extent of mapped mesohabitats associated with a flood (i.e., habitat stability), I rescanned a 32 km portion (67%) of the study area on May 22, 2013 when river discharge at Chattahoochee was 623 m^3s^{-1} (22,000 f^3s^{-1}). This post-flood sonar dataset was processed and mesohabitats were digitized and classified according to previously described methods.

To assess change, the post-flood May 2013 mesohabitat map was superimposed on the original March 2012 map; each map was converted to a raster dataset with a 1 m^2 pixel (cell) grid. To quantify differences between the two maps, I used the Raster Calculator tool in the ArcToolbox; this tool provides a rapid algorithm for quantifying differences in pixel values between two raster datasets. Differences in pixel values were interpreted as areal changes, and were summarized and organized in a matrix to aid in interpretation (Congalton & Green 2008). I refer to the results of this GIS-based analysis as "raw change". To calculate the percentage of change that occurred to each mesohabitat I divided the change in area within each class by the total area of the class prior to the flood (i.e., the March 2012 map). Areas where bedform had changed from smooth/plane to rippled or duned, and vice versa, after the flood were interpreted as unstable, and not likely to be suitable habitat for mussels.

A certain amount of positional error is inherent in any sonar-based habitat map due to GPS accuracy experienced during the sonar survey (Kaeser and Litts 2010; 2012). Moreover, when rescanning a reach of river, it is likely the boat will follow a path that deviates slightly from that taken during a previous survey. Since the path of the boat determines the position of the water column and, therefore, the aforementioned displacement of features within the

imagery, it is possible that feature boundaries delineated in imagery from two separate surveys could produce variable results in a change detection framework. In this study, I define areal differences between two maps attributable solely to navigation and GPS positioning as "mapping error". I recognized the influence of mapping error on the quantification of post-flood, raw areal changes, and deemed it necessary to estimate these error rates.

To estimate mapping error, sonar image datasets collected during identical field conditions were required. Two simultaneous surveys were conducted along a 15 km portion (30.9%) of the study area on August 8th, 2013 at discharges of 566 m^3s^{-1} (20,000 f^3s^{-1}) using two survey vessels equipped with separate Humminbird 1198c sonar systems. This approach ensured that the field conditions (i.e., bedforms and depths) that each sonar system experienced were identical, and therefore any differences between the resulting maps would be due solely to mapping error. Each sonar image set was processed and classified by the author resulting in two classified polygon layers representing the same mesohabitat classes observed during identical field conditions. The total area of each mesohabitat class measured from the first map was divided by the total area of each mesohabitat class measured from the second map in order to calculate the net proportion of change in habitat area between the two maps. The percentage of change in area that occurred in each mesohabitat class between the two maps was calculated and interpreted as a net range of percent error (Congalton & Green 2008). The range of percent error per mesohabitat class was compared to the net percent change in area that occurred between the pre and post flood habitat maps.

In addition to the mapping error assessment, areas identified as having changed after the flood were visually inspected to verify whether bedform had truly changed, or whether changes were simply due to variation in how the boundary lines were drawn. If a physical change in

bedform was evident in an area of change, the polygon representing the area was classified as having passed visual inspection. Areas of change occurring as a result of boundary line alignment (i.e., mapping error) were classified as having failed visual inspection. A matrix summarizing all verified physical changes (i.e., "verified change") was prepared to compare to results from the GIS-based analysis (i.e., raw change) and the mapping error assessment.

Results

The resulting, classified mesohabitat map encompassed approximately 700 ha of river channel inundated at a low flow of 141.5 m^3s^{-1} (5,000 f^3s^{-1}). The map contained 203 mesohabitat patches distributed among 50 consecutive meander bends (i.e., sites). With few exceptions, each site contained one representative of each mesohabitat class (Table 2; Figure 6; Figure 7). The smallest mesohabitats on average were the Inner and Outer Recirculation Zone (mean area per site = 5,500 and 3,400 m^2, respectively), while the Pool/Outer Bank habitat units averaged 20,000 m^2 in area. Together, the Inner and Outer Recirculation Zones represented 6.2% of the total habitat area, while Point Bar and Mid-Channel mesohabitat classes composed 77.9% of the total area. Pool/Outer Bank mesohabitats represented the remaining 15.0% within the study area.

In terms of relative composition, the habitat classes associated with smooth bedforms typically represented between 15% and 25% of the total area of each site (Figure 9). Sites 28-39 located between rkm 67 and 80 (i.e., RM 41.8 to 50) appeared to be geomorphically different from other sites. These sites occupied smaller areas and contained larger proportions of smooth bedform habitat (>25%) compared to other sites throughout the study reach. Sites 28-39 are also associated with a section of the study reach that had the lowest water surface slope (Figure 10).

Results of the mesohabitat change analysis revealed a majority of the mapped areas remained unchanged after a 10-year flood event (Table 3). Areas exhibiting the largest amount of raw change occurred between Mid-Channel habitat boundaries. The raw change analysis indicated that Inner and Outer Recirculation Zone mesohabitats increased in area post flooding, whereas the percent in Pool/Outer Bank mesohabitats decreased (Table 4).

Ranges of percent change due mapping error exceeded the net percent raw change detected from pre and post flood maps for all mesohabitats except the Pool/Outer Bank. Net percent mapping error showed highest variability in the Inner and Outer Recirculation Zones (15.9% and 15.6%, respectively; Table 4). Mapping area was low in both the Pool/Outer Bank (+/- 1.2), and Mid Channel (+/- 0.02) mesohabitats.

Area of verified post-flood changes to bedforms exceed mapping error only within the Pool/Outer Bank mesohabitat class. All other mesohabitat classes had smaller percentages of verified change than their associated mapping error. The largest verified changes occurred at the Mid-Channel and Pool/Outer Bank interface (Table 5) with a decrease of 4.9% in total Pool/Outer Bend habitat area due to Mid-Channel encroachment. Verified percent decreases in the Inner and Outer Recirculation Zone mesohabitat areas due to Mid-Channel encroachment were -1.5% and -4.1%, respectively (Table 6). Inner Recirculation Zone habitat was verified to increase by 0.76%. A small percentage (0.9%) of the Inner Recirculation Zone was changed to Point Bar habitat, and 0.4% of the Mid-Channel exhibited change to the Pool/Outer Bank habitat.

Discussion

The results of the sonar based mapping effort show that this habitat classification for freshwater mussels exhibited distinct repeatable units across the entire 700 ha study area.

Moreover, the average habitat areas produced from the bedform-based classification system support the meso-scale definitions I designated in this study (Frissel et al. 1986; Newson and Newson 2000).

Additional features contributed to the identification of mesohabitat boundaries among adjacent habitats exhibiting similar smooth bedforms. In particular, submerged large woody debris served as a reliable indicator of active bank erosion and the beginning of the Pool/Outer Bank mesohabitat class, and dark image tones indicating fine particle deposition were useful for distinguishing the Inner and Outer Recirculation zones from the Pool/Outer Bank. Dark tones indicative of fine sediments were often variable within the Inner and Outer Recirculation mesohabitats, indicating that these mesohabitats likely contained a variety of fine-grained, surficial substrates. Tonal heterogeneity within Inner and Outer Recirculation Zones suggests that a map based solely on substrate classification would look considerably different than a map based on fluvial geomorphology and river bedform patterns.

Previous mussel studies in the Apalachicola River have assumed that Inner and Outer Recirculation Zones are stable during high flow conditions (Beidenharn, 2007; Miller and Payne, 2007; Harvey 2007), but the degree of stability was not assessed. The results of both the raw and verified areal change analyses confirmed that mesohabitat bedforms remained largely unchanged after major discharge events. Areas of smooth bedforms may thus provide stable refuge habitat for freshwater mussels during flood events. Smooth bedforms associated with flow refugia were often observed to extend > 10 m from the bank even after a flood event. These boundaries suggest potentially stable freshwater mussel habitat in the Apalachicola River actually extends quite a bit further from the bank than previous studies have suggested following analyses of transect-based mussel surveys (EnviroScience 2006a). A sonar based mesohabitat mapping

approach as presented in this study may provide more complete information on the extent of suitable freshwater mussel habitat, however sampling for mussels within these mapped mesohabitats is required to substantiate this hypothesis.

The areal extent of the Pool/Outer Bank was the second largest in total and average patch size of the five mesohabitat classes, and sonar imaging indicated a smooth/plane bed characteristic. The plane bedform in the Pool/Outer Bank was likely caused by flow velocity at the bed transitioning between the velocities that cause the characteristic dunes and ripples of the Mid Channel and Point Bar and higher velocities that form plane bedforms (Arcement and Schneider 1989; Julien and Raslan 1998). Despite encroachment of the sand dunes and ripples of the Mid Channel environment across the Pool/Outer Bank boundary, a large majority of the smooth bedform of the Pool/Outer Bank mesohabitat class remained intact after the flood disturbance. Studies of meander bend hydrodynamics suggests that high shear stress in this environment during high flows leads to sediment transport, scouring, and deepening of this habitat (Garcia et al. 2012; Leopold and Wolman 1960), and hydraulic conditions occurring on the outer bank in the Pool/Outer Bank mesohabitat class during floods are erosive and powerful, causing the felling of large trees growing close to the bank. Large aggregations of submerged woody debris were clearly imaged in the Pool/Outer Bank mesohabitat class, with some aggregations > 100 m in length and extending > 20 m across the channel. Extensive aggregations of large woody debris may deflect flow during floods (Abbe and Montgomery 1996), and possibly create favorable microhabitat refuge conditions for mussels during high flows within the Pool/Outer Bank mesohabitat.

In previous studies, Kaeser and Litts (2008, 2010) examined the classification or thematic accuracy of sonar-based habitat maps. In this study I assumed that my ability to differentiate

smooth from rippled or duned bedforms was highly accurate, as these characteristics were highly observable and boundaries between the two bedform types were highly distinct throughout the study area. Verification of boundaries as discrete transitions between zones of differing hydrologic conditions by empirical measurement of hydrologic variables was beyond the scope of this study. Verification of boundaries by direct underwater observation was, likewise, logistically unfeasible. Moreover, based on the results of the change analysis, I would not expect boundaries to remain perfectly static between a sonar survey occurring at higher flows and the execution of a groundtruthing operation that required divers and lower flow conditions. Such temporal shifts in the position of boundaries between adjacent mesohabitats could lead to co-registration errors, and confound an assessment of mesohabitat classification accuracy (Congalton and Green 2008). Rather than attempt a traditional, classification accuracy assessment of mesohabitats, I conducted an assessment of mapping error rates, a type of error I defined previously as resulting from both survey navigation and GPS positional error.

Observed changes in habitat after the 10-year flood event could have been due in part to mapping error. The results of the mapping error assessment allowed me to infer levels of variation associated with areal estimates in the map. For example, estimates of Inner Recirculation Zone area varied by 15.9% between two maps of the same area and conditions. Therefore, the estimate of total available Inner Recirculation Zone habitat in the study area (207,733 m^2) may vary by as much as +/- 33,030 m^2. However, the net change in Inner Recirculation Zone area I observed between pre and post flood habitat maps was only 13,805 m^2, leading to the conclusion that net changes detected in the pre and post flood maps might be largely attributed to mapping error, highlighting the need to verify stability by visually inspecting sonar imagery.

Both change due to mapping error and actual changes to the bedforms were incorporated in the results of the raw change analysis. I deemed it necessary to determine the extent of these two potential sources of change by visually inspecting the sonar imagery to confirm the change was due to either mapping error or due to a visible change in bedform pattern, and results indicated that even less habitat change actually occurred in the Inner and Outer Recirculation Zone mesohabitats. Indeed, most of the verified changes to bedform occurred due to encroachment of the Mid Channel into smooth bedform habitats that could possibly be suitable for mussels. Even though some new Inner and Outer Recirculation Zone mesohabitats were verified to form after the flood, these newly formed habitats were likely not yet occupied by mussels. In other words, newly formed smooth bedform may not necessarily represent quality, suitable habitat for mussels. A portion (4.9%) of the Pool/Outer Bank mesohabitat was verified to change from smooth bedform to ripple and dune that typically occurred along the Mid Channel boundary line, and often involved large aggregations of woody material being covered by a mass of sand dune and ripples (Figure 11).

The success of using complex hydraulic variables to predict freshwater mussel distribution and abundance strongly suggest temporal fluctuations in river flow dynamics play an integral part of the persistence of freshwater mussel populations (Strayer 1999, Morales 2006, Steuer et al. 2008, Allen and Vaughn 2010). Parasiewicz et al. (2012) used an intensive survey of hydraulic characteristics across a large spatial extent and over variable flow conditions to calibrate a mesohabitat-scale predictive model of optimal freshwater mussel habitat for one species. This kind of extrapolation includes the spatial extent considerations and temporal variability needed for management of freshwater mussels at the meso-scale, but there is still a need to develop cost effective and efficient strategies for gathering such data across larger spatial

extents and other riverine systems in order to identify, quantify, and quickly preserve critical habitat of these imperiled species. The approach taken in this study facilitated a rapid classification of large, turbid river habitats and confirmed the bedform stability associated with 3 of 5 habitat units.

The high repeatability of this mesohabitat classification could be applied to rivers of similar meandering geomorphology and alluvial sediment transport characteristics as boundaries between the presented mesohabitat classes were easily identified in sonar imagery in predictable locations, and were also supported by research of hydrologic patterns occurring around meandering river bends (Garcia et al. 2012). The results of this study suggested that time-lapse sonar imaging may provide a cost-effective, alternative means of assessing habitat stability for freshwater mussels in sand-bed rivers. To the best of my knowledge, this study is the first to demonstrate the use of low-cost side-scan sonar mapping to detect and quantify reach-level changes in benthic habitat conditions in a large river system over a wide spatial extent.

II. Predicting the distribution and abundance of the freshwater mussel *Amblema neislerii* in a middle reach of the Apalachicola River, Florida

Introduction

Mapping and modeling the distribution and abundance of freshwater mussel species in large turbid rivers is challenging. Large rivers frequently include deep-water habitats that are difficult to access, and sampling across large spatial extents is logistically demanding. In some cases this leads to surveys that are limited in scope and inference. However, because many freshwater mussel taxa are endangered, threatened or of special concern in the United States and Canada (Williams et al. 1993), development of practical, efficient techniques to reveal their distribution and monitor population trends remains a high priority.

Species distribution models (SDMs) are increasingly being used to predict suitable habitat for organisms over large spatial extents (Guisan and Zimmerman 2000). Advances in geographic information systems (GIS), remote sensing, and computer processing have contributed to the success of SDMs in the management of species habitat, modeling of species distribution for conservation planning, and assessment of management actions (Guisan and Thuiller 2006). SDMs applied to freshwater mussel ecology have been used to guide conservation activities (Prie et al. 2012), and can be useful to explain the distribution of mussels across multiple scales of study (Newton et al. 2008).

Sampling of freshwater mussels is often limited by time and funding constraints. In spite of the aforementioned challenges associated with sampling mussels in large rivers, accurate habitat data are required for use of SDMs (Guisan and Thuiller 2005). Recent work in the upper Mississippi River used historical data and hydraulic modeling to explain the distribution and

abundance of freshwater mussels with high accuracy across a 30-km reach (Morales et al. 2006; Steuer et al. 2008; Zigler et al. 2008; Allen & Vaughn 2010). This work suggested that freshwater mussel distribution and abundance was controlled by the stability of benthic conditions during high discharges. However, deriving the complex hydraulic variables necessary for such predictions require technical expertise and resources that may limit the widespread adoption of this approach. Therefore, the development of low-cost, less technical approaches to model freshwater mussel distribution in large turbid rivers remains a worthy goal toward advancing the conservation of this imperiled group of organisms.

The Apalachicola River in northwest Florida is a large alluvial river of the Southeast Coastal Plain that is recognized as a biodiversity hotspot (Blaustein 2008), and has drawn considerable conservation attention due to intensive demands on its water resources (Light et al. 2002). The river supports a high diversity and abundance of freshwater mussels, including the federally endangered Fat Threeridge (*Amblema neislerii)* (Brim Box and Williams 2000). A restricted range, perceived threats associated with channel modifications and water management, and patchy habitat distribution were cited as factors contributing to *A. neislerii*'s listing as endangered under the Endangered Species Act in 1998 (Federal Register 1998). Efforts led by the U.S. Fish and Wildlife Service (USFWS) to recover the species have been guided by strategies outlined in the Service's Recovery Plan (USFWS 2003). Recent survey work has provided estimates of *A. neislerii* population size in the Apalachicola River (EnviroScience 2006a; Miller and Payne 2007; Gangloff 2012), but estimates vary considerably among studies. Such differences are likely due to variations in sampling methodology that, in turn, influence perspectives on abundance and habitat associations. The current perspective of *A. neislerii* distribution and abundance suggests most mussels reside in shallow waters, however there has

been no concerted effort to systematically sample deep water habitats in the Apalachicola River (EnviroScience 2006a; Miller and Payne 2006; Gangloff 2012; USFWS 2012).

Dense aggregations of *A. neislerii*, and other freshwater mussels, have consistently been located along river margins directly downstream of point bars in several Apalachicola River studies (Brim Box & Williams 2000, EnviroScience 2006a; Gangloff 2012). These habitats are described as moderately depositional and remaining stable during floods (Miller and Payne 2007; Harvey 2007; Beidenharn 2007; Chapter 1). Although commonly targeted during surveys, only the upstream and downstream boundaries of these habitats have been georeferenced. Mapping of moderately depositional habitats using review of aerial photographs and field reconnaissance to identify riparian features such as point bars, willow stands, and bank slope inflection points to delimit habitat boundaries was conducted by the USFWS in 2008 (Gangloff 2012). Prior to my investigation, however, the actual underwater boundaries of these habitats remained unknown. Deep water habitats in the Apalachicola River, including the Pool/Outer Bank and Mid Channel mesohabitats (Chapter 1) have not been heavily sampled in past survey work, due to the hazards associated with deep water, swift currents and numerous submerged trees (EnviroScience 2006b; Miller and Payne 2007). These critical data gaps limit both the reliability of current *A. neislerii* population estimates and the perception that this species primarily occupies shallow, moderately sloping, near-bank habitats (EnviroScience 2006a; Gangloff 2012; USFWS 2012).

A recent study designed to assess the impact of water-level drawdown on *A. neislerii* populations in moderately depositional habitats yielded *A. neislerii* population estimates for these habitats throughout the Apalachicola River and the lower Chipola River, a large tributary (Gangloff 2012). Abundance estimates were intended to be minimum population estimates for the system, and inferences regarding the potential impacts to *A. neislerii* populations associated

with river level management by the U.S. Army Corps of Engineers (USACE) were incorporated in a recent Biological Opinion produced by the USFWS (2012). Both Gangloff (2012) and other recent studies (EnviroScience 2006a) reported the occurrence *A. neislerii* in deep-water habitats, suggesting a more comprehensive survey of *A. neislerii* distribution and abundance in the Apalachicola River is needed to generate accurate population estimates to guide river management and species recovery.

Sonar habitat mapping of benthic features in the Apalachicola River identified patches of stable habitat that were larger and more numerous than prior studies of *A. neislerii* have indicated (Chapter 1). Habitat classification revealed that the habitat classes corresponding to previously known *A. neislerii* aggregations may be more numerous and more extensive, and revealed similarities between moderately depositional and poorly-surveyed deep-water habitats. In this study, I used the habitat classification map developed in Chapter 1 to guide a stratified, quantitative survey of *A. neislerii* across a 50 km reach of the Apalachicola River. I developed predictive species distribution models of *A. neislerii* presence/absence as well as abundance using only habitat boundaries and variables derived from my sonar-based map.

Methods

Study Area

The Apalachicola River is a large alluvial river formed by the confluence of the Chattahoochee and the Flint Rivers at river navigation mile 106 directly below the Jim Woodruff Lock and Dam Reservoir at the Georgia/Florida state boundaries (Figure 1). Below Jim Woodruff Lock and Dam the Apalachicola River flows unimpeded for 170 km to the Gulf of Mexico. Along its course the channel geomorphology changes considerably allowing clear

dissection of the river into upper, middle, and lower-non tidal zones (Light et al. 2006). The upper section is a relatively straight channel composed predominantly of coarse sand and gravel with scattered limestone outcroppings that continue until river kilometer (rkm) 130, the point at which the surrounding geology drops from the Tallahassee Hills to the Coastal Lowlands (Harvey, 2007; Florida Geological Survey). At this transition into the middle reach, the channel geomorphology begins to exhibit a strong meandering characteristic with elevated sinuosity, and sediment composition changes to primarily coarse and fine sand. At rkm 67, a side channel known as the Chipola cut-off connects the Apalachicola River to the Chipola River, a large tributary, and serves as a landmark to the beginning of the lower non-tidal reach.

I chose the section of the Apalachicola River with the greatest sinuosity and most repetitive meandering pattern as my study area, beginning at rkm 104 and ending at a point of observable straightening of the channel at rkm 56, just below "Sand Mountain", a large aggregation of sand spoils visible on the bank created from historical dredging. This area includes most of the middle reach as defined by Light et al. (2006) and Gangloff (2012), as well as an upstream portion of the lower-non tidal reach.

Freshwater Mussel Survey

Sampling Approach

A sonar-based mesohabitat map produced for the study area was used to stratify the sampling of freshwater mussels (Chapter 1). Mesohabitat classes of this map represented patches of common geomorphology, flow, and bedform characteristics occurring in meander bends. Several classes suspected to support freshwater mussel populations were identified as stable during a post-flood change analysis, while other classes represented depositional and/or turbulent

environments commonly associated with large alluvial rivers. Stratification is highly recommended for freshwater mussel surveys in which a priori habitat information is available (Strayer & Smith 2003), and is also useful when allocating limited time and monetary resources across broad spatial extents with costly sampling techniques such as SCUBA. In this study, a stratified approach served to quantitatively assess hypothesized mussel/habitat associations within the meandering, middle reach of the Apalachicola River and perhaps elucidate the factors contributing to the high density of *A. neislerii* populations in this reach.

Rather than randomly selecting sampling locations from mesohabitats throughout the entire study area, I decomposed the study area into a series of 50 consecutive study sites using reference boundaries drawn between the downstream end of each Inner Recirculation Zone and the downstream end of the Outer Recirculation Zone on the opposite side of the channel. With few exceptions, each site was composed of one representative of each mesohabitat class, or five mesohabitats. Six of these sites were selected for sampling by first grouping the 50 sites into six groups of approximately equal numbers of consecutive sites (i.e., eight or nine sites per group), and then using a random number generator to select one sampling site from each of the six groups. This approach ensured that sampling sites would be distributed throughout the 50 km reach.

Next, I assigned 10 sampling points to each mesohabitat class occurring in each of the six sampling sites using the Generalized Random Tessellated Stratification (GRTS) sampling algorithm found in the spsurvey package (Kincaid and Olsen 2013) for the R software platform. This algorithm randomly generates a set of points that are distributed in a spatially balanced manner within a user-defined extent, thereby decreasing probabilities of bias and auto-correlation (i.e., clumping of points). The GRTS points are ordered, and consecutively distributed in a way

that preserves the spatial balance of the set, so that if one point cannot be sampled, the sampling crew can target the next ordered point in the set; this point will be spatially balanced among the rest.

Sampling points were located in the field with a Garmin GPSmap 760CSx GPS unit and immediately marked with an anchored buoy. A set of geographic coordinates representing the actual sampling location was recorded, and a 1.78-m length of metal cable representing the radius of a 10-m^2 sampling plot was attached to a piece of rebar inserted vertically into the river bed at the center of the sampling plot (Ghent et al. 1978, Gregoire and Valentine 2007). The radial cable was used to delimit the extent of the sampling plot, and tactile searches were conducted by 2-5 crew members to remove all mussels present in the plot. All freshwater mussels were identified to species and enumerated; a measurement along the longest axis of any *A. neislerii* <50 mm was recorded. The depth at the center of the plot, and a classification of the predominant substrate type within the plot was recorded. Predominant substrate was classified as either 1) coarse sand, 2) fine sand, 3) a mixture of fine sand, silt, and mud, or 4) other. Due to preponderance of unoccupied sites in the Mid-Channel mesohabitat class and the hazardous nature of SCUBA sampling in this high velocity and unstable substrate environment, I reduced the number of plots sampled in this mesohabitat from 6 to 3 plots per site.

Data Analysis

One-way ANOVA was used to test for differences between *A. neislerii* counts and mesohabitat classes. Two species distribution models were developed for *A. neislerii*. The first was a presence/absence model based on a multiple logistic regression with a binomial distribution, and the second was a count model using multiple generalized linear model (GLM)

regression. I used a negative binomial error distribution (log link) to model counts per sampling plot because *A. neislerii* counts were not normally distributed (Davis et al. 2013). I fit the models in R 3.1 (R Development Core Team 2012) using the MASS package (Venables & Ripley 2002) function glm( ) for the presence/absence models and the glm.nb( ) function for the count models. A set of candidate models was developed using different combinations of six explanatory variables that represented alternate hypotheses regarding factors that influence *A. neislerii* presence/absence or abundance in the Apalachicola River. I considered the following explanatory variables: mesohabitat class, rkm, distance to the 141.5 m^3s^{-1} (5,000 f^3s^{-1}) river bank, distance to nearest unstable mesohabitat (i.e. shortest distance to Point Bar or Mid-Channel), water depth, and substrate type.

To derive explanatory variables, GPS coordinates of the sampled locations were loaded into the ArcGIS 10.2 (ESRI 2013) software platform and metrics were generated using analysis tools in the ArcToolbox. The mesohabitat map was used to associate each sampling location with the mesohabitat class in which the plot occurred (Chapter 1). For each sampling location, the shortest distance to the 141.5 m^3s^{-1} river bank, and the distance to nearest unstable habitat were calculated using the NEAR analysis tool in ArcToolbox. Each sampling location was associated with the nearest tenth of a river kilometer. Data obtained from the field survey, including mussel counts, sampling plot depth, and predominant substrate type were integrated with the resulting table of habitat metrics, and this composite database was exported as a comma separated value (.csv) file. The data table was loaded into the R software platform for statistical analysis and model development.

To determine which variables or sets of variables were most important in explaining *A. neislerii* presence/absence and counts per sampling plot I used an information-theoretic (IT)

model selection approach (Kullback and Leibler 1951; Kullback 1959). The IT approach is an evidence-based model selection technique useful for investigating complex ecological hypotheses (Anderson 2008). Performance of models was ranked according to the Akaike information criterion corrected for small sample size (AIC_c) along with model weights, and model summaries were reported for the presence/absence as well as abundance models with the lowest AIC_c value. The area under the curve (AUC) metric was computed for the best performing presence/absence model as a measure of accuracy. Specificity (true negative) and sensitivity (true positive) rates were also computed for the best performing presence/absence model and plotted with estimated probabilities of occurrence in order to find the optimal probability (i.e., the 'cutpoint') in which both rates were maximized. Predicted probabilities greater than or equal to the optimal cutpoint were considered presences and all observations with probabilities less than the optimal cutpoint were considered absences.

When developing the count model, I decided to remove all sampling points occurring in the Point Bar and Mid Channel mesohabitat classes based on the very low probabilities associated with *A. neislerii* occurrence in these two habitats. The fit and accuracy of the most informative abundance model was assessed by calculating the regression coefficient (R^2) from a linear regression between observed and predicted counts of *A. neislerii* at the sampling plot level (Pineiro et al. 2008), and points were tested for correlation using a Pearson correlation test. Residuals were plotted to assess model fit.

To generate an estimate of the total abundance of *A. neislerii* in the middle reach using the predictive capacity of most informative count model, I first overlaid a raster grid on the study area with a cell size equal to the actual mussel sampling area used in this study (10 m^2). A point was assigned to the centroid of each cell in the grid, and each point was attributed unique values

for each of the habitat variables included in the most informative abundance model. Because the Point Bar and Mid-Channel observations were not included in the development of the count model, all points of the grid located within the Mid-Channel and Point Bar mesohabitats were removed from the dataset, leaving ~150,000 points covering the Inner and Outer Recirculation Zone and the Pool/Outer Bank mesohabitat classes. The point data table was imported in R, and the prediction function of the MASS package was used to predict the abundance of *A. neislerii* at each point using the most informative count model. The sum total of predicted abundances provided a raw estimate of the number of *A. neislerii* occurring across the entire study area.

When predicting abundance across a landscape, practitioners should consider the ranges associated with predictor variables, and exercise caution when attempting to predict outside of the range of values inherent in the model (Guisan and Thuiller 2006). In other words, a model should not be used to extrapolate beyond the information used to build it. When examining preliminary results of predicted abundance in specific regions of the map, particularly those associated with areas close to the river banks in the Pool/Outer Bend mesohabitat, I noticed unrealistically high values (>1,000 mussels/m^2). These values exceeded the maximum count observed during the field survey, and were associated with the predictor "nearest distance to unstable habitat" that exceeded the range of values in the sample set used to develop the model. Therefore, I removed all GIS-generated prediction points with values outside the range of model set variables. The remaining predictions at each point across the landscape were summed to provide an "adjusted" reach wide population estimate of *A. neislerii*.

Verifying the accuracy of predicted abundance

Although it was beyond the scope of this study to conduct additional field sampling to evaluate the accuracy of abundance model predictions, an independently-derived data set was available from recent sampling conducted by Gangloff (2012) in my study area. These data enabled me to compare and contrast density and abundance estimates made using two different, quantitative approaches at both site and reach scales, and to identify primary factors associated with differences in abundance estimates. This sampling approach involved 5-6 transects originating at, and oriented perpendicular to, the bank at each sampling site (Gangloff 2012). A suction dredge was used to excavate consecutive, 0.25-m^2 quadrats along each sampling transect. The use of a suction dredge, although time-consuming, is considered both quantitative and highly effective at capturing mussels present within a sampling frame (Strayer and Smith 2003). Sites sampled by Gangloff (2012) were randomly selected from a set of suitable mussel sites whose upstream and downstream boundaries had been defined prior to this investigation. Gangloff's (2012) set of suitable sites were located within the Inner and Outer Recirculation Zone mesohabitat classes mapped in this study.

The spatial data associated with sampling sites, in combination with reported transect measurements, allowed me to generate and overlay polygons in the habitat map representing the approximate areas sampled by Gangloff (2012). I used these polygons to extract my model-based estimates of abundance at each of the sampling sites for an analysis of congruency between the two estimates at the site scale. Gangloff (2012) provided a reach-wide estimate of *A. neislerii* abundance by multiplying the total length of all available mussel sites by the average number of mussels estimated to occur per longitudinal meter of sampled sites. To derive a comparable, reach-wide estimate from the count model, I used the coordinates of all available mussel sites and the average length of all transects sampled by Gangloff within my study area to generate a

set of equivalent polygons, and used these polygons to extract the corresponding model-based estimates from my abundance map.

Results

I sampled a total of 164 radial plots each 10 m^2 for a total area sampled of 1640 m^2. A total of 3958 individual *A. neislerii* were collected. *Amblema neislerii* was the 3rd most abundant mussel among species collected, comprising 34.5% of the total mussels collected. Juvenile *A. neislerii* $\leq$ 30 mm represented 5.4% of the total collection, and 2.2% of *A. neislerii* were $\leq$ 20 mm.

Significant differences ($P < 0.0001$) were found between mesohabitat classes and *A. neislerii* counts per sample plot (Figure 12). Nearly all (99.3%) *A. neislerii* were found within 21% of the study area consisting entirely of smooth bedform signatures in sonar imagery (Inner and Outer Recirculation Zones, Pool/Outer Bank; Table 8). *Amblema neislerii* were notably absent from sampling locations in the ripple and dune bedform mesohabitats. Approximately 80% of the sampling plots were unoccupied within the Point Bar mesohabitat class and only 1 sampling plot was occupied in the Mid Channel. *Amblema neislerii* was found at a maximum depth of 8.5 m, and a maximum of 37.1 m from the edge of the 141.5 m^3s^{-1} bank. The maximum *A. neislerii* density observed was 43.4 mussel/m^2.

A dramatic increase was observed in site-level *A. neislerii* density from 0.5 mussels/m^2 at site 19 (rkm 85), to 5.3 mussels/m^2 at site 29 (rkm 75). Site density remained relatively high at the two sites downstream (rkm 68 and 60; Figure 9). Although observed maximum densities among the different mesohabitat classes peaked at different sites, the trend in mean density of the

Outer Recirculation Zones closely resembled the overall average site density trend across the study area (Figure 9).

Of the six top ranking presence/absence models, there was strong support for the model that included the explanatory variables of mesohabitat class, rkm, and distance to low flow bankline (Table 9). Two models comprising a small proportion of AIC weight included the additional variables of distance to unstable habitat and water depth. The AUC of the top ranked presence/absence model was 0.939, with an optimal cutoff probability for predictions occurring at 0.7 (Figure 14). No observations within the Point Bar and Mid Channel habitats (n=62) had greater than a 70% chance of *A. neislerii* occurrence. Coefficient estimates of the top ranked presence/absence model indicated that all smooth bedform mesohabitat classes were positively associated with the presence of *A. neislerii* (Table 10). The Mid Channel mesohabitat class was negatively associated with the species presence. Model coefficients for rkm and distance to low-flow bankline indicated that habitats located further upstream, or further from the bank had lower likelihoods of *A. neislerii* occurrence. The probability of *A. neislerii* occurrence ($\hat{\pi}_i$) was represented by the most informative multiple logistic regression model in the following equation:

$$\hat{\pi}_i = \frac{\exp(\beta_0(Point\ Bar) + \beta_1(Inner\ Recirculation\ Zone) + \beta_2(Outer\ Recirculation\ Zone) + \beta_3(Pool\ Outer\ Bank) + \left(-\beta_4(Mid\ Channel)\right) + (-\beta_5(rkm)) + (-\beta_6(Distance\ to\ low\ flow\ bank)))}{1 + (\exp(\beta_0(Point\ Bar) + \beta_1(Inner\ Recirculation\ Zone) + \beta_2(Outer\ Recirculation\ Zone) + \beta_3(Pool\ Outer\ Bank) + \left(-\beta_4(Mid\ Channel)\right) + (-\beta_5(rkm)) + (-\beta_6(Distance\ to\ low\ flow\ bank))))}$$

The count model set showed the top ranked model to be the single most parsimonious model with a model weight of 0.99 (Table 11). The top ranked model contained variables of mesohabitat class, rkm, distance to low-flow bankline, and distance to unstable habitat, while models that included variables of substrate type and water depth had little support (Table 11). For the top ranked abundance model, rkm and distance to low-flow bankline had a negative

relationship with *A. neislerii* counts, whereas distance to unstable habitat had a positive effect on *A. neislerii* counts (Table 12). The number of *A. neislerii* per $10m^2$ sampling point was represented by the most informative count model in the following equation:

$$\ln(\#\widehat{A.neislerii_i}) = \begin{array}{c}\beta_0(Inner\ Recirculation\ Zone) + \beta_1(Outer\ Recirculation\ Zone) + \\ \beta_2(Pool\ Outer\ Bank) + \left(-\beta_3(rkm)\right) + \\ \left(-\beta_4(Distance\ to\ low\ flow\ bankline)\right) + \left(-\beta_5(Distance\ to\ unstable\ habitat)\right)\end{array}$$

Observed and predicted numbers were significantly correlated ($P < 0.001$). The regression coefficient (R^2) between the observed number and predicted number from the highest ranked count model was 0.34, and the slope of the regression line equaled 0.85 (Figure 15). The scatterplot of residuals between observed versus predicted *A. neislerii* contained normal variability. Two outliers were identified in the plot; one outlier involved an observation of 434 mussels and a model prediction of 86 mussels, and the other outlier involved a prediction of 351 mussels relative to an observation of 230 mussels (Figure 15).

Amblema neislerii population estimate

The most informative count model generated an estimate of 8,687,083 *A. neislerii* within the 700 ha study reach. This included an estimated 1,178,708 mussels in the Inner and Outer Recirculation Zones combined, and an estimated 7,508,375 mussels in the Pool/Outer Bank mesohabitat class. The area of prediction included only the Inner and Outer Recirculation Zone area, and 89.7 % of the Pool/Outer Bank mesohabitat class. The excluded portion of the Pool/Outer Bank (118,020 m^2) represented areas primarily near the river banks that fell outside of the range of predictor variables used to build the model.

Comparisons with an independent dataset

The average *A. neislerii* density observed in this survey within Inner and Outer Recirculation Zone mesohabitat classes was 4.1 mussels/m^2, while the average *A. neislerii* density sampled previously was 4.9 mussels/m^2 across 12 Inner and Outer Recirculation Zone sites within my study area (Gangloff 2012). At the site level, I found no correlation between *A. neislerii* abundance estimates from the count model and corresponding estimates made by Gangloff (2012; Figure 11). The count model over-estimated the number of *A. neislerii* estimated by Gangloff (2012) at several sites, but also underestimated the number existing at a few sites by a greater magnitude. This trade-off resulted in a count model based, total estimate of *A. neislerii* occurring within Gangloff (2012) sampling sites of 81,907 mussels, a number somewhat lower than estimated by Gangloff (2012) (n= 86,335). Likewise, when examining only the exact same areas considered by Gangloff (2012) as 'potential' habitat that fell within my study area, my reach wide estimate of numbers of *A. neislerii* (n= 175,124) was lower than Gangloff's (2012) estimate of 199,679 mussels.

Area of potential *A. neislerii* habitat varied widely between what I identified with sonar mapping and what Gangloff (2012) identified (Figure 13). Gangloff's (2012) potential habitats covered 46,455 m^2 over 43 sites within my study area, while the sonar habitat map of Inner and Outer Recirculation Zones covered 429,880 m^2 across 101 mesohabitat patches (Table 10). Thus, the sonar habitat mapping approach identified twice as many sites and ten times more area than previously identified by field reconnaissance and inspection of areal imagery (Figure 12). Gangloff's (2012) maximum sampled depth was reported as 2.25 m, and maximum transect length (distance from bank) was 15.0 m, while I sampled to a maximum depth of 4.6 m and a

maximum distance to the bank of 22.4 m within Inner and Outer Recirculation Zone mesohabitats. In these habitats, *A. neislerii* was collected in 12 of 12 sampling plots occurring at depths greater than the maximum sampled by Gangloff (2012), and in 4 of 7 plots occurring at greater distances to the bank than sampled by Gangloff (2012).

Species distribution map

The results of predicted probabilities of *A. neislerii* occurrence and abundance when displayed in a spatial context revealed highest probabilities and abundances occurring near and parallel to the bank (Figure 18; Figure 19). Areas were predicted probabilities were < 0.7 did occur within the Inner and Outer Recirculation Zones and the Pool/Outer Bank mesohabitat classes, and were located near the edge adjacent to the Mid Channel (Figure 18; Figure 20). Points with predicted probabilities of < 0.7 were considered unoccupied areas, composing 20% of the smooth bedform mesohabitat areas. The Pool/Outer Bank mesohabitat class displayed a larger area of high (> 100 mussels per 10-m^2 cell) predicted abundances than in the Inner and Outer Recirculation Zones (Figure 21).

Discussion

The results of this study profoundly alter existing paradigms of *A. neislerii* distribution in the middle reach of the Apalachicola River. The species had been previously described as primarily inhabiting shallow, near bank habitats where stable substrates existed (EnviroScience 2006a; Beidenharn 2007; Harvey 2007; Miller and Payne 2007; USFWS 2012). This association raised major concerns for population-level impacts due to stranding and mortality associated with river level fluctuations (i.e., manipulated draw down rates; EnviroScience 2006a; USFWS

Biological Opinion 2012), and motivated additional research to assess levels of vulnerability (Gangloff 2012). With respect to the inner and outer recirculation zones traditionally surveyed for *A. neislerii*, I have determined that these stable mesohabitats were not only larger and more numerous than previously described, but that *A. neislerii* regularly occupied greater depths and further distances from the bank in this reach of the Apalachicola River. I mapped nearly 10 X the amount of suitable inner and outer recirculation zone habitat than was previously considered when Gangloff (2012) estimated abundance in the study reach.

Amblema neislerii is not restricted to shallow water and channel margin habitats as previously thought, and therefore populations may be more resilient to reductions in water level. EnviroScience (2006a) reported most *A. neislerii* sampled quantitatively were found at depths $\leq$ 1 m, and Miller and Payne (2007) found *A. neislerii* to depths of 2.7 m, while the USFWS Biological Opinion (2012) reported *A. neislerii* sampled up to a depth of 5 m in moderately depositional as well as moderately erosional habitats, but stated that a majority of the population occurred at depths of 1 m. In contrast, 56% of the total *A. neislerii* collected in this study occurred at depths $\geq$ 1.0 m. *Amblema neislerii* was found in five sampling points with depths greater than 5 m, and to a maximum depth of 8.5 m. In addition to greater depths, *A. neislerii* was also found in greater distances from the bank than other studies. Gangloff (2012) found *A. neislerii* to a distance of 22.4 m from the bank, whereas the maximum distance from the bank of a sample containing *A. neislerii* was 37.1 m in this study.

Furthermore, large numbers of *A. neislerii* were regularly documented in a habitat not well sampled in past studies- the Pool/Outer Bank mesohabitat class. Little is known about *A. neislerii* populations living in this habitat, and the high rate of occupancy observed in the Pool/Outer Bank habitat was unexpected. *Amblema neislerii* was found at depths between 2.3-

8.5 meters in the Pool/Outer Bank, and the average density in this habitat was nearly equal to the densities of the Inner and Outer Recirculation Zones. Because the Pool/Outer Bank mesohabitat class covers such a large area, the potential number of *A. neislerii* existing in this mesohabitat class is likely substantial. The total habitat area of the Pool/Outer bank may have been underestimated due to the 2-dimentional nature of sonar habitat mapping. The steep bank slope of the Pool/Outer Bank habitat exists as a 3-dimentional environment, and consequently the 2-D sonar habitat map did not quantify the 15-30ft vertical face of the outer bank. Interestingly, EnviroScience (2006a) identified the upper portions of moderately-erosional, steep banks adjacent to deep (~20 ft) water as 1 of 3 primary habitats where *A. neislerii* were found in highest abundance. The authors also noted the occurrence of the species in deep water adjacent to steep banks, but suggested mussels occurred there because they were dislodged from the upper bank. The vertical wall of the outer bank was not properly quantified in the map, and no sampling points were randomly assigned to the bank wall, causing a portion of *A. neislerii* habitat area to be excluded from this study.

Hydrodynamic forces occurring within the Pool/Outer Bank habitat in meander bends may explain how *A. neislerii* is able to survive embedded in the bank material. As water flows around a steeply banked meander bend, secondary flow patterns develop close to the bank that decrease the sheer stress acting upon the upper portions of the vertical face that thereby decreasing scouring forces and erosion (Bathurst et al. 1979; Blanckaert 2011; Garcia et al. 2012). Meanwhile the lower portions and the horizontal bed experience mostly primary flows causing high shear stresses that are responsible for the erosional nature and smooth plane bedform used to classify the Pool/Outer Bend. However, 1/3 of observations in the Pool/ Outer Bank reported fine particle substrate types (Figure 22), which suggest the hydrodynamic

conditions within the Pool/Outer Bank habitat area are not uniformly erosional and that deposition of fine particles does occur at many locations within this habitat at some point in the hydrodynamic cycle. Research on seasonal variation in hydrodynamic conditions in thalweg environments suggests that these environments may experience a shift from erosional at higher flows to depositional at slower flows (Keller 1971; Thompson et al. 1999; MacWilliams et al. 2006). The effect of large woody material may also be responsible for local deposition of finer sediments observed in many Pool/Outer Bank sampling points (Figure 23). Large woody material can deflect flows during floods, cause deposition of sediments, stabilize banks, and provide habitat for many aquatic organisms (Mutz, 2000; Abbe and Montgomery, 1996; Thompson 1995; Gurnell et al. 1995). EnviroScience (2006a) found *A. neislerii* living next to large woody material located 20-30 m from the bank, and many Pool/Outer Bank observations in this study reported large woody material occurring within the sampling point area. Although I did not attempt to quantify the amount of large woody material in the study area, large aggregations of woody material were easily identified in sonar imagery (Figure 24), and previous research has demonstrated that large woody material can be quantified using side scan sonar (Kaeser and Litts 2008). Indeed, large woody material aggregations were sometimes too dense to sample with SCUBA safely, causing some sampling points to be skipped, and possibly causing bias towards sampling areas with less woody material. Juvenile mussels were also located in this habitat, including the largest collection of juvenile *A. neislerii* among any sampling point (38 < 20 mm). The high occupancy rates and variety of size classes among the sampling points in the Pool/ Outer Bank habitat class (26 of 29) provides strong evidence that this habitat class contains suitable habitat conditions for *A. neislerii*.

Sampling results are consistent with the assumed unsuitable nature of the Point Bar and Mid Channel mesohabitat classes, as a very small portion of sampling points within these classes were found to contain only a few individuals. The small numbers of *A. neislerii* occurring in the Point Bar mesohabitat class is not surprising due to the close proximity and upstream location of adjacent habitat classes that held large numbers of *A. neislerii* (Outer Recirculation Zone, Pool/Outer Bank). Mussels could move short distances or perhaps be displaced from the upstream habitats across boundaries to the Point Bar. One observation in the Mid Channel habitat contained 9 *A. neislerii*, but this sampling location was < 1 m from an Outer Recirculation Zone boundary. GPS error alone (3 – 5 m) could have resulted in a misplacement of the sample point just outside of the mesohabitat actually sampled in the survey. Although fewer points were sampled in the Mid Channel than other habitat types, only one sampling point contained *A. neislerii*, and this point was located < 1 m from the Outer Recirculation Zone. Based on these results, I do not believe additional sampling in the Mid Channel would detect mussels in this unstable habitat.

The increase in total suitable habitat area estimated in this study resulted in an increased estimate of population abundance in middle reach of the Apalachicola River. By simply multiplying habitat area by the average *A. neislerii* density sampled per habitat class (i.e. the approach taken in Gangloff 2012), the number of *A. neislerii* in this study was estimated to be an order of magnitude greater than previous estimates. However, this simple estimate does not address the variability likely occurring within habitat classes and among sites, and a more comprehensive model would provide a more accurate total population estimate.

The species distribution models developed in this study used relatively simple and easily derived habitat metrics obtained from sonar-based habitat maps and GIS software, and provide

more detail on factors associated with *A. neislerii* distribution and abundance in the Apalachicola River. Distance to the 141.5 m^3s^{-1} (5,000 f^3s^{-1}; "low flow") bank, distance to unstable habitat, and rkm were all generated post survey, and the inclusion of these variables in the most informative models suggests these metrics are associated with relevant ecological phenomena controlling *A. neislerii* distribution and abundance.

Distance to the low flow bank was found in the most informative of both presence/absence and count models, suggesting that as distance to the water's edge at low flow increases, the likelihood of mussel occurrence and abundance decreases. Previous studies have also reported a decline in *A. neislerii* occurrence and abundance as distance to the wetted edge increases (EnviroScience 2006a; Gangloff 2012). Relationships between *A. neislerii* occurrence and abundance and distance to low flow bank measured in this study were important in the most informative models primarily because I conducted all sampling during a period of 141.5 m^3s^{-1} (5,000 f^3s^{-1}) river flow conditions that represent the minimum water level currently regulated in the Apalachicola River. If the wetted edge of the river had been defined at higher flows and sampled during a period of greater discharge, the distance to bank relationship may not be as strong as measured in this survey. Receding flows force *A. neislerii* and other mussels residing near the water's edge to relocate to lower elevations or face desiccation (USFWS 2012, unpublished data), and consecutive periods of seasonally low flows could eventually shift the distribution of mussels to lower elevations. Surveys that do not consider the history of flows with respect to the location of mussels in the channel might falsely conclude mussels don't exist or are at lower densities in locations near the bank if sampling takes place in areas that were exposed during recent low flow periods.

Distance to unstable habitat as an influential habitat metric effecting *A. neislerii* abundance was supported by the most informative count model. Results of the areal change analysis performed in Chapter 1 provided evidence to explain why this variable was significant within stable habitats. The Mid Channel habitat was composed of migrating sand dunes and was observed to shift to some extent across the boundaries of smooth bedform and stable habitats (Inner and Outer Recirculation Zone, Pool/Outer Bank) after a 10-year flood event. Mussels residing near such a boundary could face dislodgement, burial, or be forced to migrate when boundaries between stable and unstable bed conditions change. Guisan and Thuiller (2005) identified distance to disturbances as a main influence on species distribution in general, and recommended such metrics to be included in SDMs if statistically supported.

The inclusion of rkm in the most informative of both presence/absence and count models suggested a longitudinal trend in *A. neislerii* distribution and abundance, with *A. neislerii* densities remaining relatively low in the three upstream sample sites (sites 8, 12, and 19) and then increasing dramatically at the remaining downstream three sites (site 29, 38, 46; Figure 13). The trend of total *A. neislerii* density per sampling site (i.e., rkm) shows a spike at rkm 75 (site 29; river navigation mile 46). Gangloff (2012) observed a similar increase in *A. neislerii* density between rkm 75 - 67 (river navigation mile 46-39). To some extent, increases in abundance in downstream directions is consistent with river ecology theory such as the river continuum concept (Vannote et al. 1980). As the meandering characteristic of the river supports the formations of stable, suitable habitat (Garcia et al. 2012), and the cumulative availability of such habitat increases in the downstream direction, so too might the densities of *A. neislerii* in response to patterns of suitable habitat availability. Alternatively, the marked increase in densities of *A. neislerii* observed within the reach between rkm 70 and 80 in this study and in

Gangloff (2012) may be the result of slower water velocities due to a flattening of elevation gradient that would increase concentration and retention time of both nutrients and larval mussels in recirculating and depositional environments. A decrease in gradient would slow water velocities and decrease the distance required for water to change direction around a meander bend, resulting in smaller sites. This is supported with lower than average mesohabitat areas occurring at a similar location on the river as a marked flattening of gradient (Figure 8; Figure 10), and a shortening of meander bend length is visible in the map of the study area (Figure 1). Locations of lower gradient and slowed water velocities could also increase the settlement of glochidia entrained in the transport mechanism of fine particulates (Morales et al. 2006). Large slough-like embayments also occurred in this section of the study area, which could provide a substantial amount of biological enrichment to downstream and adjacent habitats. Off-channel habitats such as sloughs and tributary mouths were not sampled because they were not included in the sonar habitat map, however, past studies have encountered *A. neislerii* living in slough and off-channel environments (Payne and Miller, 2002; EnviroScience 2006a).

Water depth and substrate type provided no additional explanatory power in the most informative models, suggesting *A. neislerii* presence/absence and abundance is only weakly related to these commonly-measured parameters. In contrast to previous reports of a significant association between water depths and abundances (EnviroScience 2006a; Gangloff 2012), *A. neislerii* was found across a range of depths and model AIC_c values support the hypothesis that water depth is less important to *A. neislerii* distribution and abundance. Like water depth, *A. neislerii* was found in a variety of substrate types. These findings indicate that an attempt to characterize suitable mussel habitat using substrate alone would not have succeeded in this river reach (Strayer and Ralley 1993; Brim Box et al. 2002; Strayer 2004). The model results indicated

that mesohabitat class was a stronger explanatory measure than substrate type, and all occupied classes exhibited a heterogeneous substrate composition (Figure 23).

Using the explanatory variables I derived with sonar and GIS analysis tools to develop models for predicting *A. neislerii* occurrence and abundance across our study area was a primary objective of this study. The most informative presence/absence model predicted 18% of the study occupied, all of which was located within smooth bedform mesohabitat classes. Although the abundance model only included the smooth bedform mesohabitat classes, not all areas within the smooth bedform mesohabitat classes were predicted to contain at least one mussel, and a map of predicted abundances clearly indicated variation across mesohabitats. Predicted abundances at the site level exhibited an increasing trend in the downstream direction (Figure 22). This effect is most likely due to influence of the rkm variable on estimates of abundance at downstream study sites. A marked increase in the estimated abundance at all sites downstream of the site with the highest observed average density (site 29) exemplified the effect of rkm on predicted *A. neislerii* abundance (Figure 22). No significant increase in suitable habitat areas was observed at lower study sites (Figure 8), further suggesting the rkm variable is largely responsible for the trend in predicted abundances.

Assessments of within model performance revealed strengths and some weaknesses of the models developed in this study. The most informative presence/absence model contained low type I and II error when predicting occurrences (Figure 14), and therefore provided a statistically accurate predictive species distribution model for *A. neislerii* presence/absence at the 10 m^2 scale in this reach of the Apalachicola River. Regression analysis between predicted abundances by the most informative count model and the observed counts from the survey were significantly correlated, however a R^2 of 0.34 suggests the accuracy of the count model needs improvement.

The geospatial map of abundance that resulted from the population estimate procedure allowed me to validate the count model predictions with data collected from an independent study conducted by Gangloff (2012). Predicted abundances estimated to occur within equal areas of Gangloff (2012) sampling sites were uncorrelated with Gangloff's (2012) estimates (Figure 16), indicating that variables not included in the count model may improve prediction accuracy at the sub-mesohabitat or site level. The inclusion of additional variables such as slope, sinuosity, or radius of curvature may improve the accuracy of count model estimates, and may result in estimates at the site-level scale that are more comparable to Gangloff's (2012). For example, *A. neislerii* densities have been shown to be highest between rkm 75 – 67, and this area exhibits distinctly less gradient (Figure 10), shorter site length (Figure 8), and contains a greater proportion of smooth bedform area per site than sites upstream and downstream (Figure 9). Using hydrogeomorphic variables associated with these observations should be incorporated in future count models to investigate potential improvements in model accuracy.

A closer inspection of where the count model estimated greater numbers of *A. neislerii* than Gangloff (2012) revealed four of these sites were occurring below a natural side channel known as the Chipola Cutoff at rkm 65. Gangloff (2012) observed low *A. neislerii* density at several sites below this feature. Further investigation revealed dredging activities for navigation channel maintenance conducted by the USACE was heavily concentrated in several areas directly below the Chipola Cutoff until a moratorium in 2001 (USACE Dredging Report 2001, unpublished data). However, even though the single site sampled below the Chipola Cutoff contained less *A. neislerii* than sites sampled upstream, the observed decrease in *A. neislerii* density was not great enough to influence the modeled relationship between the variable rkm and mussel density, and consequently caused predicted abundance to steadily increase below the

Chipola Cutoff (Figure 23). The combination of Gangloff's (2012) data, USACE dredging locations, and knowledge of shallow channel bathymetry led me to consider the removal of study sites 41, 42, 48, and 50 below the Chipola Cutoff from the population estimate. This removed nearly 1,500,000 mussels from the initial population estimate for a final adjusted estimate of 7,132,332 *A. neislerii* potentially living in the study area.

Although my final population estimate greatly exceeds previous estimates, this estimate may, in fact, remain conservative. In addition to fully excluding four sites, 118,020 m^2 of the Pool/Outer Bank habitat was removed from prediction. Furthermore, the tactile sampling technique used in this survey may have missed some of the smallest individuals. Gangloff (2012) sampled 4.5x as many juvenile *A. neislerii* less than 30mm using a suction dredge as found using tactile searches alone in this study, and therefore observed densities in this study may be slightly less than true density. However, searching with tactile methods in this study still uncovered 221 *A. neislerii* less than 30mm in length, representing 5.6% of the total population sampled, and leads to the conclusion that the sampling method used in this study was still effective at capturing juveniles and detecting recruitment.

Population estimates from Gangloff (2012) and this study were similar, but I estimated dramatically higher numbers of *A. neislerii* in recirculation habitats when using the full extent of suitable habitat area identified with side scan sonar. The discrepancy in population estimates is primarily due to the difference in estimated suitable habitat area between the studies. All of Gangloff's (2012) sample sites that occurred in my study area were in the Inner and Outer Recirculation Zones. However, I quantified total Inner and Outer Recirculation Zone habitat area to be an order of magnitude greater than that of Gangloff (2012), and consequently the total

number of *A. neislerii* estimated in recirculating habitats was also an order of magnitude greater (Table 13).

The paradigm shift in *A. neislerii* habitat use and population sizes occurring as a result of this study provides an example of how differences in study methodology can significantly effect estimates of population size and critical habitat. Peterson et al. (2001) reviewed three independent studies that assessed the magnitude of environmental degradation to coastal habitats from a large oil spill, and found that differences in sampling approaches were responsible for polarized conclusions of the extent of damage to natural resources. Sonar habitat mapping was employed in this study to identify the extent of difficult-to-access habitats and this information was used to stratify sampling efforts for an endangered freshwater mussel. Results show that this population may be less prone to extinction than previously thought, and it is possible that an integrated, sonar-based study approach could identify previously unrecognized habitat for other freshwater mussel populations in systems similar to the Apalachicola River.

The sonar-based habitat classification employed in this study corresponds to areas of stable habitat as measured by complex hydraulic variables in other large alluvial river systems. Zigler et al. (2008) created a geospatial model with estimates of substrate stability in a 30-km reach of the Upper Mississippi River and found areas of the mid channel that contained large sand dunes exhibited high sediment mobility rates and therefore were unstable and shifting, while channel margins in sinuous reaches were identified as areas with high probabilities of mussel presence and high abundance. Past studies have shown a high degree of correlation between stable habitats and mussel abundance (Strayer 1999; Morales et al. 2006; Steuer et al. 2008; Allen & Vaughn 2010), and large meandering rivers support the formation and maintenance of stable habitats adjacent to the bank at the inflection points of meander bends

(Klienhans et al. 2010). Stable habitats that provide flow refuge from flood disturbances have been associated with high probability of juvenile settlement, whether through presence of fish hosts (Vaughn and Taylor 2000) or depositional hydrology (Morales et al. 2006), and correspond directly to the Inner and Outer Recirculation Zones identified in this study. Areas where flow recirculates increases residence time of nutrients that can contribute to higher benthic invertebrate diversity and richness (Garcia et al. 2012; Townsend et al. 1989; Vannote et al. 1980), and can also increase the residency time of fish hosts and food required for freshwater mussel populations to persist (Strayer 2004).

To my knowledge, this is the first study to use side scan sonar to classify potential mussel habitat across a large river reach, and then use map-derived variables to model distribution and abundance at this scale. The entire 700 ha study area was scanned, mapped, and sampled for freshwater mussels within one year, further supporting the utility of this study's methodology for limited budget and time constricted situations. A similar approach involving mapping potential habitat first, stratifying samples accordingly, and modeling with the resulting data might also alter ecological perspectives on other freshwater mussel species in large rivers as this study has done for *A. neislerii*.

Conclusion

Identifying the spatial extents of freshwater mussel habitats with side scan sonar habitat mapping has considerably revised the perspective on Fat Threeridge (*Amblema neislerii*) distribution and abundance in the Apalachicola River. Using bedforms to delineate habitats at the mesoscale and using time lapse sonar image analysis to confirm habitat stability provided a low cost, efficient approach to focus efforts to sample *A. neislerii* across this 50 km reach of the

Apalachicola River. The sampling approach taken in this study revealed *A. neislerii* residing in undistinguished habitats and occupying greater extents than previously recognized, and sonar-based and GIS-derived habitat variables were sufficient to develop species distribution models to estimate population size over large spatial extents. The information gained from this study has identified previously unrecognized suitable habitat, and provided a more comprehensive perspective of *A. neislerii* distribution and abundance. I believe the integration of low-cost, sonar habitat mapping, stratified mussel surveys, and species distribution modeling may help fill a critical gap in information necessary to study and manage these imperiled organisms in a variety of other river systems.

References

Abbe, T., Montgomery, D.R. 1996. *Woody debris jams, channel hydraulics and habitat formation in large rivers.* Regulated rivers: Research and Management, Vol. 12, 201-221.

Anderson, D.R. 2008. *Model Based Inference in the Life Sciences: A Primer on Evidence*. Springer Press.

Anima, Roberto, Wong, Florence L., Hogg, David, and Galanis, Peter, 2007, Side-scan sonar imaging of the Colorado River, Grand Canyon: U.S. Geological Survey Open-File Report 2007-1087, 15 p.

Allen, D.C., and Vaughn, C.C., 2010. *Complex hydraulic and substrate variables limit freshwater mussel species richness and abundance.* Journal of the North American Benthological Society 29(2):383-394.

Arbuckle, K.E., and Downing, J.A., 2002. *Freshwater mussel abundance and species richness: GIS relationships with watershed land use and geology.* Canadian Journal of Aquatic Science 59: 310-316.

Arcement, Jr., G.J., Schneider, V.R., 1989 *Guide for Selecting Manning's Roughness Coefficients for Natural Channels and Floodplains:* United States Geological Survey Water-supply Paper 2339.

Bathurst, J.C., Hey, R.D., Throne, C.R. 1979. *Secondary flow and shear stress at river bends.* Journal of the Hydraulics Division. Vol. 105. No. 10 pp 1277-1295

Biedenharn, D.S. 2007. Cursory Geomorphologic Evaluation of the Apalachicola River in Support of the Jim Woodruff Dam Interim Operations Plan. USACE Summary of Findings.

Blanckaert, K. 2011. *Hydrodynamic processes in sharp meander bends and their morphological implications*. J. Geophys. Res. 116, F01003, doi: 10.1029/2010JF001806

Blaustein, R.J. 2008. *The Florida Pandhandle: Biodiversity Hotspot*. BioScience 58:784-790.

Bovee, K.D., Waddle, T.J., Bartholow, J., and Burris, L., 2007, A decision support framework for water management in the upper Delaware River: U.S. Geological Survey Open-File Report 2007-1172, 122 p.

Box, B. B., Dorazio, R.M., Liddell, W.D., 2002. *Relationships between streambed substrate characteristics and freshwater mussels (Bivalvia: Unionidae) in coastal plain streams.* Journal of the North American Benthological Society 21(2): 253-260

Box, B.B., Williams, J.D. 2000. *Unionid Mollusks of the Apalachicola Basin in Alabama, Florida, and Georgia.* Bulletin of the Alabama Museum of Natural History. 21:1-143.

Brainwood, M., Burgin, S., Byrne, M., 2008. *The role of geomorphology in substratum patch selection by freshwater mussels in the Hawkesbury-Nepean River (New South Wales) Australia.* Aquatic Conservation Marine and Freshwater Ecosystems 18: 1285-1301.

Coffman, D.K., Malstaff, Greg, and Heitmuller, F.T., 2011, *Characterization of geomorphic units in the alluvial valleys and channels of Gulf Coastal Plan rivers in Texas, with examples from the Brazos, Sabine, and Trinity Rivers.* 2010: U.S. Geological Survey Scientific Investigations Report 20011-5067, 31 p.

Congalton, R.G., Green, K. 2008. *Assessing the Accuracy of Remotely Sensed Data: Principles and Practices, Second Edition.* CRC Press.

Davis, E. A., David, A. T., Marie Norgaard, K., Parker, T. H., McKay, K., Tennant, C., Soto, T., Rowe, K., Reed, R. 2013. *Distribution and Abundance of Freshwater Mussels in the mid Klamath Subbasin, California*. Northwest Science. Vol. 87, No. 3.

Dietrich, W. E., Smith, J.D., Dunne, T. 1979. *Flow and Sediment Transport in a Sand Bedded Meander.* The Journal of Geology, Vol. 87, No. 3, pp. 305 – 315.

DiMaio, J., Corkum, L.D. 1995. *Relationship between the spatial distribution of freshwater mussels (Bivalvia: Unionidae) and the hydrologic variability of rivers.* Canadian Journal of Zoology. 73: 663-671

Elliot, C.M., Jacobson, R.B., DeLonay, A.J. 2004. *Physical Aquatic Habitat Assessment, Fort Randall Segment of the Missouri River, Nebraska and South Dakota.* USGS Open-File Report 2004-1060.

EnviroScience, Inc. 2006a. *Freshwater Mussel and Habitat Surveys of the Apalachicola River, Chipola River and Selected Sloughs/Tributaries.* Report for the Florida Department of Environmental Protection. USFWS Archives. Doc. No. 176. Pp 2110 – 2214.

Federal Register. 1998. "*ETWP; Determination of Endangered Status for Five Freshwater Mussels and Threatened status for Two Freshwater Mussels From the Eastern Gulf Slope Drainages of Alabama, Florida, and Georgia*". 63 FR 12664 12687.

Fausch, K. D., Torgersen, C.E., Baxter, C.V., Li, H. W. 2010. *Landscapes to Riverscapes: Bridging the Gap between Research and Conservation of Stream Fishes*

Frissel, A.C., Liss, W.J., Warren, C.E., Hurley, M.D., 1986. *A Hierarchical Framework for Stream Habitat Classification: Viewing Streams in a Watershed Context.* Environmental Management Vol. 10, No. 2, pp. 99-214.

Furguson, R.I., Parsons, D.R., Lane, S.N., Hardy, R.J. 2003. *Flow in meander bends with recirculation at the inner bank.* Water Resources Research. 39 (11). p. 1322.

Gangloff, M. 2012. *Population size and depth distribution of three federally-protected mussels in the Apalachicola and Lower Chipola rivers.* Southeastern Aquatic Research Report for the U.S. Army Corps of Engineers.

Garcia, X.F., Schnauder, I., and Pusch, M.T., 2012. *Complex hydromorphology of meanders can support benthic invertebrate diversity in rivers.* Hydrobiologia 685: 49-68.

Ghent, A.W., Singer, R., Johnson-Singer, L. 1978. *Depth distributions determined with SCUBA, and associated studies of the freshwater unionid clams Elliptio complanata and Anodonta grandis in Lake Brenard, Ontario*. Can. J. Zool. 56:1654-1663.

Gregoire, T.G., Valentine, H.T. 2007. *Sampling Strategies for Natural Resources and the Environment*. CRC Press. 496 p. Chapter 7, pages 207 – 246.

Guisan, A.G., Thuiller, W. 2005. *Predicting species distribution: offering more that simple habitat models*. Ecology Letters 8:993-1009.

Gurnell, A., Gregory, K., Petts. G. 1994. *The role of coarse woody debris in forest aquatic habitats: implications for management*. Aquatic Conservation: Marine and Freshwater Ecosystems. 5:143-166.

Harvey, M.D. 2007. *Cursory Fluvial Geomorphic Evalution of the Apalachicola River in Support of the Jim Woodruff Dam Interim Operations Plan: Summary of Findings*. Mussetter Engineering, Inc.

Hastie, L.C., Boon, P.J., Young, M.R. 2000. *Physical microhabitat requirements of freshwater pearl mussels, Margaritifera margartitifera (L.).* Hydrobiologia 429: 59-71.

Hawkins, C.P., Kershner, J.L., Bisson, P.A., Bryant, M.D., Decker, L.M., Gregory, S.V., McCullough, D.A., Overton, C.K., Reeves, G.H., Steedman, R.J., Young, M.K. 1993. *A Hierarchical Approach to Classifying Stream Habitat Features.* Fisheries, 18:6, 3-12

Julien, P.Y., Raslan, Y. 1998. *Upper Regime Plane Bed.* Journal of Hydraulic Engineering. Vol 124. No. 11. Pp 1086.

Kaeser, A.J., Litts, T.L., and Tracey, T.W., 2012. *Using low-cost side scan sonar from benthic mapping throughout the lower Flint River, Georgia, USA.* River Research and Applications 10.1002/rra.

Kaeser, A.J., Litts, T.L., 2010. *A novel technique for mapping habitat in navigable streams using low-cost side scan sonar.* Fisheries 35: 163-174.

Keller, E. A., 1971. *Areal sorting of bed-load material: the hypothesis of velocity reversal*. Geological Society of America Bulletin 82: 753–756.

Kincaid, T.M., Olsen, A. R. 2013. Spsurvey: Spatial Survey Design and Analysis. R package version 2.6. URL: http://www.epa.gov/nheerl/arm/.

Klienhans, M.G., Blanckaert, K., McLelland, S.J., Uijttewaal, W.S.J., Murphy, B.J., van de Kruijs, A., Parsons, D. 2010. *Flow Separation in Sharp Meander Bends.* Proceedings of the HYDRALAB III Joint User Meeting, Hannover, February 2010.

Kullback, S., Leibler, R. A. 1951. *On information and sufficiency.* Annals of Mathematical Statistics 22, 79-86.

Kullback, S. 1959. *Information theory and statistics*. John Wiley, New York, NY.

Leopold, L.B., Wolman, M.G., 1960. *River Meanders.* Geological Society of America Bulletin. 71. No. 6. Pp 769-793.

Levin, S. A. 1992. *The Problem of Pattern and Scale in Ecology*. Ecology. 73(2). pp. 1943-1967

Light, H.M, Darst, M.R., and J.W. Grubbs. 1998. *Aquatic Habitats in Relation to River Flow in the Apalachicola River Floodplain, Florida*. U.S. Geological Survey Professional Paper 1594. ISBN 0-607-89269-2.

Light, H.M., Vincent, K.R., Darst, M.R., and Price, F.D., 2006. *Water-Level Decline in the Apalachicola River, Florida, from 1954 to2004, and Effects on Floodplain Habitats:* U.S. Geological Survey Scientific Investigations Report 2006-5173, 83 p., plus CD.

MacWilliams, M.L., Jr., Wheaton J.M., Pasternack, G.B., Street, R.L., Kitanidis, P.K. 2006. *Flow convergence routing hypothesis for pool-riffle maintenance in alluvial rivers.* Water Resour. Res., 42, W10427, doi:10.1029/2005WR004391.

Manley, P.L., Singer, J.K., 2007. *Assessment of sedimentation processes from side-scan sonar surveys of the Buffalo River, New York, USA.* Environmental Geology. DOI 10.1007/s00254-007-1109-8

McRae, S.E., Allan, J.D., and Burch, J.B., 2004. *Reach- and catchment-scale determinants of the distribution of freshwater mussels (Bivalvia: Unionidae) in south-eastern Michigan, U.S.A.* Freshwater Biology 49: 127-142.

Miller, A.C, Payne, B.S. 2006. *The fat threeridge (Amblema neislerii), the surprisingly common endangered mussel in the Apalachicola River, Florida*. Gale Opposing Viewpoints in Context.

Miller, A.C., Payne, B.S. 2007. *Factors determining abundance and distribution of the Endangered Fat Threeridge mussel, Amblema neislerii, in the Apalachicola River*.

Morales, Y., Weber, L.J., Mynett, A.E., Newton, T.J., 2006. *Effects of substrate and hydrodynamic conditions on the formation of mussel beds in a large river.* Journal of the North American Benthological Society 25(3): 664-676

Mutz, M. 2000. *Influences of woody debris on flow patterns and channel morphology in a low energy, sand bed stream reach.* International Review of Hydrobiology 85: 107-121.

Newton, T., Woolnough, D. A., Strayer, D.L. 2008. *Using landscape ecology to understand and manage freshwater mussel populations.* Journal of the North American Benthological Society. 27(2):424-439.

Nitsche, F.O., Ryab, W.B.F., Carbotte, S.M., Bell, R.E., Slagle, A., Bertinado, C., Flood, R., Kenna, T., McHugh, C. 2007. *Regional patterns and local variations of sediment distribution in the Hudson River Estuary.* Estuarine, Coastal and Shelf Science 71 259-277

Padmore, C.L. 1998. *The role of physical biotopes in determining the conservation status and flow requirements of British rivers.* Aquatic Ecosystem Health & Management. Vol. 1, Issue 1

Parasiewicz, P., Castelli, E., Rogers J.N., Plunkett, E., 2012. *Multiplex modeling of physical habitat for endangered freshwater mussels.* Ecological Modeling 228: 66-75

Payne, B.S., Miller, A.C. 2002. *Mussels Associated With Floodplain Channels Connected to the Apalachicola River.* USACE Environmental Laboratory Report. ERDC/EL TR-02-13.

Peterson, C.H., McDonald, L.L., Green, R.H., Erickson, W. P. 2001. *Sampling design begets conclusions: the statistical basis for detection of injury to and recovery of shoreline communities after the 'Exxon Valdez' oil spill*. Marine Ecology Progress Series. Vol. 210; 255-283.

Peterson, J.T., Rabeni, C.F. 2001. *Evaluating the Physical Characteristics of Channel Units in an Ozark Stream.* Transactions of the American Fisheries Society, 130:5, 898-910.

Phillips, Jonathan D., 2008. *Geomorphic Units of the Lower Sabine River*. Project Report for the Texas Water Development Board and Texas Instream Flow Program.

Pineiro, G., Perelman, S., Guerschman, J.P., Paruelo, J.M., 2008. *How to evaluate models: Observed vs. predicted or predicted vs. observed?* Ecological Modelling. 216 pp. 316-322.

Prie, V., Molina, Q., Gamboa, B. 2013. *French naiad* (Bivalvia: Margaritiferidae, Unionidae) *species distribution models: prediction maps as tools for conservation.* Hydrobiologia. DOI 10.1007/a10750-013-1597-3.

Statzner, B. Gore, J.A., Resh V.H. 1988. *Hydraulic stream ecology: observed patterns and potential applications.* Journal of the North American Benthological Association 7, 307-60

Steuer, J.J., Newton, T.J., Zigler, S.J., 2008. *Use of complex hydraulic variables to predict the distribution and density of unionids in a side channel of the Upper Mississippi River*. Hydrobiologia 610: 67-82.

Strayer, D.L., Ralley, J. 1993. *Microhabitat use by and assemblage of stream dwelling unionaceans (Bivalvia), including two rare species of Alasmidonta*. Journal of the North American Benthological Society. 12: 247-258.

Strayer, D.L., and D.R. Smith. 2003. A guide to sampling freshwater mussel populations. American Fisheries Society, Monograph 8, Bethesda, Maryland.

Strayer, D.L. 2008. *Freshwater Mussel Ecology: A Multifactor Approach to Distribution and Abundance*. University of California Press. Freshwater ecology series volume 1.

Strayer, D.L. 1999. *Use of flow refuges by unionic mussels in rivers.* Journal of the North American Benthological Society. 18(4):468-476.

Strayer, D.L., Malcom, H.M., Bell, R.E., Corbotte, S.M., and Nitsche F.O., 2006. *Using geophysical information to define benthic habitats in large river.* Freshwater Biology 51: 25-38.

Thompson, D. 1995. *The effects of large organic debris on sediment processes and stream morphology in Vermont.* Geomorphology. 11:235-244.

Thompson, D.M., Wohl, E.E., Jarrett, R.D. 1999. *Velocity reversals and sediment sorting in pools and riffles controlled by channel constrictions.* Geomorphology 27(1999) 229-241.

Townsend, C. R. 1989. *The patch dynamics concept of stream community ecology.* Journal of the North American Benthological Society. 8(1):36-50.

U.S. Fish and Wildlife Service (USFWS). 2003. United State Fish and Wildlife Service Recovery plan for endangered fat threeridge (*Amblema neislerii*), shinyrayed pocketbook (*Lampsilis subangulata)*, Gulf moccasinshell (*Medionidus penicillatus*), Ochlockonee moccasinshell (*Medionidus simpsonianus*), and oval pigtoe (*Pleurobema pyriforme*); and threatened Chipola slabshell (*Elliptio chipolaensis*), and purple bankclimber (*Elliptoideus sloatianus*). Atlanta, Georgia.

U.S. Fish and Wildlife Service (USFWS). 2012. Biological Opinion on the U.S. Army Corps of Engineers, Mobile District, Revised Interim Operating Plan for Jim Woodruff Dam and the Associated Releases to the Apalachicola River. Prepared by the U.S. Fish and Wildlife Service Panama City Field Office, Florida. 166 p.

Vannote R.L., Minshall, G.W., Cummins, K.W., Sedell, J.R., Cushing, C.E. 1980. *The River Continuum Concept*. Canadian Journal of Fisheries and Aquatic Sciences. 37.1980, pp130-137.

Vaughn, C.C., Taylor, C.M. 2000. *Macroecology of a host-parasite relationship.* Ecography. 23:1.

Venables. W.N., Ripley, B.D. 2002. Modern Applied Statistics with S. Fourth Edition. Springer, New York. ISBN 0-387-95457-0

Wiens, J.A. 2002. *Predicting species occurances: progress, problems, and prospects.* In: *Predicting species occurances: Issues of accuracy and scale* (eds Scott, J.M., Heglund, P.J., Morrison, M.L., Haufler, J.B., Raphael, M.G., Wall, W.A., Samson, F.B.). Island Press, Covelo, CA. pp 739-749.

Weins, J.A. 2002. *Riverine landscapes: taking landcape ecology into the water*. Freshwater Biology. 47, 501-515.

Williams, J.D., Warren, M.L., Cummings, K.S., Harris, J.L., Neves, R.J. *Conservation Status of Freshwater Mussels of the United States and Canada*. Fisheries 18:9, 6-22.

Zigler, S.J., Newton T.J., Steuer, J.J., Bartsch, M.R., Sauer, J.S., 2008. *Importance of physical and hydraulic characteristics to unionid mussels: a retrospective analysis in a reach of a large river*. Hydrobiologia 598: 343-360

Tables

Table 1. Descriptions and features of the mesohabitat classification scheme.

Mesohabitat unit	Flow conditions	Bed stability & depositional pattern	Bedform pattern	Location in channel	Sonar features
Point Bar	Turbulent	Unstable; Highly depositional of coarse particles	Ripples/Dunes	Inner bend bank attached	Bright image tone, dunes and ripples
Inner Recirculation Zone	Recirculation/flow separation eddy	Stable; Moderately depositional of finer particles and organic matter	Smooth plane	Bank attached downstream of Point Bar inner bend	Smooth texture; darker image tone; moderate bank slopes-dull sonar return from edge
Outer Recirculation Zone	Recirculation/flow separation eddy	Stable; Moderately depositional of finer particles and organic matter	Smooth plane	Bank attached downstream of Pool/Outer Bend	Smooth texture; darker image tone; moderate bank slopes-dull sonar return from edge; large woody material
Mid-Channel	Turbulent	Unstable; Transport of coarse particles	Ripples/ Dunes	Center of channel	Bright image tone, dunes and ripples
Pool/Outer Bend	Unidirectional secondary flow	Stable at low flow; Erosion at high flow; Deposition of coarsest particles and submerged wood	Smooth plane	Bank attached outer portion of meander bend	Smooth texture; bright image tone; steep/verticle bank-bright sonar return from edge; large woody material

Table 2. Mesohabitat area mapping results across the study reach.

Mesohabitat Unit	Total Number of units	Average Area Per unit (ha)	Total Area (ha)	% of Total Habitat
Point Bar	49	1.03	50.6	7.3
Inner Recirculation Zone	49	0.55	27.1	3.9
Outer Recirculation Zone	49	0.34	15.7	2.3
Mid-Channel	50	10.0	498.6	71.6
Pool/Outer Bank	50	2.1	104.3	15.0

Table 3. Area in hectares and percent change occurring to each mesohabitat class after a 10 year flood event. The mesohabitat classes listed vertically on the left column correspond to the mesohabitat classes that existed preflood, and the horizontally listed mesohabitat classes on the top column correspond to the mesohabitats that existed post flood. For example, the inner recirculation zone exhibited a 3.8% change in area to the Point Bar mesohabitat after the flood event. Shaded boxes represent area and percentages that remained unchanged.

		Post-flood data				
		Point Bar	Inner Recirculation Zone	Outer Recirculation Zone	Mid-Channel[a]	Pool/Outer Bank
Pre-flood data	Point Bar	264.9 (80.3%)	2.7 (0.8%)	2.0 (0.6%)	60.2 (18.3%)	0 (0%)
	Inner Recirculation Zone	8.0 (3.8%)	167.1 (80.4%)	0 (0%)	16.7 (8.0%)	15.9 (7.7%)
	Outer Recirculation Zone	1.7 (1.5%)	0 (0%)	85.3 (71.0%)	25.5 (21.2%)	7.5 (6.2%)
	Mid-Channel	66.8 (2.1%)	38.9 (1.2%)	21.4 (0.6%)	3,023.9 (93.5%)	84.9 (2.6%)
	Pool/Outer Bank	0 (0%)	11.6 (1.5%)	11.8 (1.5%)	118.8 (15.6%)	618.8 (81.2%)

Table 4. Comparisons of the % net change between pre and post flood sonar habitat maps, and the % change that was measured from two sonar habitat maps representing identical field conditions presented here as a measure of % mapping error. The % net change that occurred between all mesohabitats except the Pool/Outer Bank fell inside the range of % error that could simply be due to differences in GPS error and path of the survey vessel.

Mesohabitat Class	Pre-flood Area (m^2)	Post-flood Area (m^2)	% Net Change	Range of % mapping error
Point Bar	329849	341760	3.6	(+/-) 5.0
Inner Recirculation Zone	207733	220818	6.3	(+/-) 15.9
Outer Recirculation Zone	120113	125915	4.8	(+/-) 15.6
Mid Channel	3235962	3245683	0.3	(+/-) 0.02
Pool/Outer Bank	760920	724421	-4.8	(+/-) 1.2

Table 5. Results of manually selecting polygons associated with a visually noticeable change in bedform pattern. Numbers are percentage of mesohabitat class on the left, vertical column that exhibited visually noticeable change in bedform to the mesohabitat class on the right, horizontal column.

		Post-flood data				
		Point Bar	Inner Recirculation Zone	Outer Recirculation Zone	Mid-Channel	Pool/Outer Bank
Pre-flood data	Point Bar		0.28	0.19	0	0
	Inner Recirculation Zone	0.95		0	1.45	0
	Outer Recirculation Zone	0	0		4.13	0
	Mid-Channel	0	0.28	0		0.44
	Pool/Outer Bank	0	0	0	4.94	

Table 6. Results of the raw change analysis for suspected stable habitat units and the Pool/Outer Bank habitat. Decrease in area due to Mid-Channel expansion is defined as the percent change that occurred from each of these habitats to the Mid Channel habitat found in Table 5 above.

Mesohabitat Unit Pre Flood	Mesohabitat unit post flood	Unverified (raw) decrease in area due to mid-channel expansion (%)	Observed percent mapping error	Verified physical area decrease due to mid-channel expansion (%)
Inner Recirculation Zone	Mid-Channel	7.6	15.9	1.5
Outer Recirculation Zone	Mid-Channel	20.8	15.6	4.1
Pool/Outer Bank	Mid-Channel	15.6	1.2	4.9

Table 7. Description and support for variables used in modeling procedure.

Variable Name	Description	Scale	Support	Source
River Kilometer	Longitudinal variable representing coarse resolution phenomena	Landscape	(Vannote et al. 1980) River Continuum Concept; Distribution of species changes from headwaters to mouths of rivers due to geomorphological and resource distribution	Point shapefile with navigation data of the Apalachicola River provided by USACE
Mesohabitat Class	Categorical variable with 5 levels representing spatially defined habitat types within the river channel	Meso	(Garcia et al. 2012) Meander bends support the formation of hydraulic refuge from flood disturbances	Sonar image maps (SIMs) and classified polygon shapefile representing mapped mesohabitats
Distance to Bank	Continuous variable representing distance to wetted edge during low flow conditions in the Apalachicola River	Meso	(Gangloff 2012) A majority of *A. neislerii* were found within short distances (<=~1 meter) of the bank	Polyline shapefile generated by digitizing edge of water from aerial photography collected during a period of low flow in the Apalachicola River
Distance to Unstable Habitat	Continuous variable representing distance to unstable migrating sand ripples and dunes associated with turbulent hydraulic conditions	Meso	(Guisan and Thuiller 2005) Distance to disturbances represents a main influence on species distribution	SIMs and mesohabitat layers representing benthic environments exhibiting a sand ripple and dune bedform
Depth	Continuous variable representing water depth of the sample point during survey	Micro	Gangloff 2012; EnviroScience 2006a found significant correlation between depths and *A. neislerii* counts	Survey data
Substrate Type	Categorical variable with 4 levels representing predominate substrate composition within each sampling plot during survey	Micro	*A. Neislerii* historically associated with substrate compositions of mixtures of fine sand and silt	Survey data

Table 8. Summary of *A. neislerii* and mesohabitat data.

Mesohabitat Class	Areal coverage within study area (m^2)	% of study area	Average *A. neislerii* density (mussels/m^2)	# of sample plots occupied/ # of plots sampled	Range of *A. neislerii* sampled per plot	*A. neislerii* count total	Average *A. neislerii* density x Area (crude estimate)	*A. neislerii* abundance model estimate
Main Channel	4,985,217	71.6	0.03	1/27	0-9	9	149,835	NA
Point Bar	505,010	7.3	0.09	7/35	0-17	30	47,961	NA
Inner Recirculation Zone	270,697	3.9	4.6	29/35	0-244	1602	1,290,186	890,246
Outer Recirculation Zone	157,183	2.3	3.7	37/38	0-434	1419	595,826	288,462
Pool/Outer Bank	1,043,241	15.0	3.1	26/29	0-230	907	3,319,052	7,508,375
Total	6,961,348			100/164		3958	5,402,860	8,687,083

Table 9. Summary of small sample size Akaike information criterion (AIC_c) ranking of *A. neislerii* presence/absence logistic models.

Rank	Variables						Δ_i	K	w_i
1	rkm	Mesohabitat Class	Distance to low flow bankline				0.0	7	0.7
2	rkm	Mesohabitat Class	Distance to low flow bankline	Distance to unstable habitat			2.2	8	0.2
3	rkm	Mesohabitat Class	Distance to low flow bankline	Distance to unstable habitat	Water depth		3.9	9	0.1
4	rkm	Mesohabitat Class					18.73	6	0.0
5		Mesohabitat Class					20.6	5	0.0
6	rkm				Water depth	Substrate Type	40.4	6	0.0

Table 10. Model summary for the AIC_c top-ranked *A. neislerii* presence/absence logistic model.

Coefficient	Estimate	SE	*Z*	*P*
(Intercept)	3.001	1.870	1.609	0.108
Inner Recirculation Zone	3.309	0.747	4.432	<0.0001
Outer Recirculation Zone	3.171	0.792	4.003	<0.0001
Pool/Outer Bank	4.600	0.937	4.907	<0.0001
Mid Channel	-0.298	1.222	-0.244	0.807
River Kilometer	-0.039	0.023	-1.706	0.088
Distance to Low Flow Bankline	-0.141	0.040	-3.574	0.0004

Table 11. Summary of small sample size Akaike information criterion (AIC_c) ranking of the *A. neislerii* abundance models.

Rank			Variables				Δ_i	K	w_i
1	rkm	Mesohabitat Class	Distance to low flow bankline	Distance to unstable habitat			0.0	6	0.99
2	rkm	Mesohabitat Class	Distance to low flow bankline	Distance to unstable habitat		Substrate Type	10.6	7	0.01
3	rkm	Mesohabitat Class	Distance to low flow bankline				21.6	5	0.0
4	rkm	Mesohabitat Class					32.5	4	0.0
5			Distance to low flow bankline	Distance to unstable habitat	Water depth	Substrate Type	46.2	7	0.0
6						Substrate Type	58.4	4	0.0
7					Water depth	Substrate Type	60.6	5	0.0
8					Water depth		62.6	8	0.0
9		Mesohabitat Class					64.47	3	0.0
10		Mesohabitat Class			Water depth		66.52	4	0.0

Table 12. Model summary for the AIC_c top-ranked *A. neislerii* abundance model using the GLM procedure with a negative binomial distribution.

Coefficient	Estimate	SE	*Z*	*P*
(Intercept)	9.750	0.809	12.05	<0.0001
Outer Recirculation Zone	-0.420	0.305	-1.38	0.167
Pool/Outer Bank	0.943	0.330	2.88	0.0040
River Kilometer	-0.082	0.009	-8.70	<0.0001
Distance to Low Flow Bankline	-0.118	0.022	-5.41	<0.0001
Distance to Unstable Habitat	0.058	0.015	3.982	<0.0001

Table 13. Comparison of sampling parameters and population estimates between Gangloff (2012) and this study.

Sampling Parameters

Methodology	Average density in inner and outer recirculation zones (mussels/m^2)	Area of potential inner and outer recirculation zone habitat in study area (m^2)	Max depth sampled in inner and outer recirculation zones (m)	Max distance from bank sampled in inner and outer recirculation zones (m)
M. Gangloff	4.9	46,455	2.25	15.0
This study	4.1	427,880	4.6	22.4

Population Estimates

Methodology	# *A. neislerii* estimated within M. Gangloff's identified potential habitat area	# *A. neislerii* estimated in inner and outer recirculation zone mesohabitat class area	# *A. neislerii* estimated within pool/outer bank mesohabitat class area	# *A. neislerii* estimated across 700 ha study area
M. Gangloff	199,679	199,679	N/A	199,679
This study	175,124	1,178,708	7,508,375	8,687,083

Figures

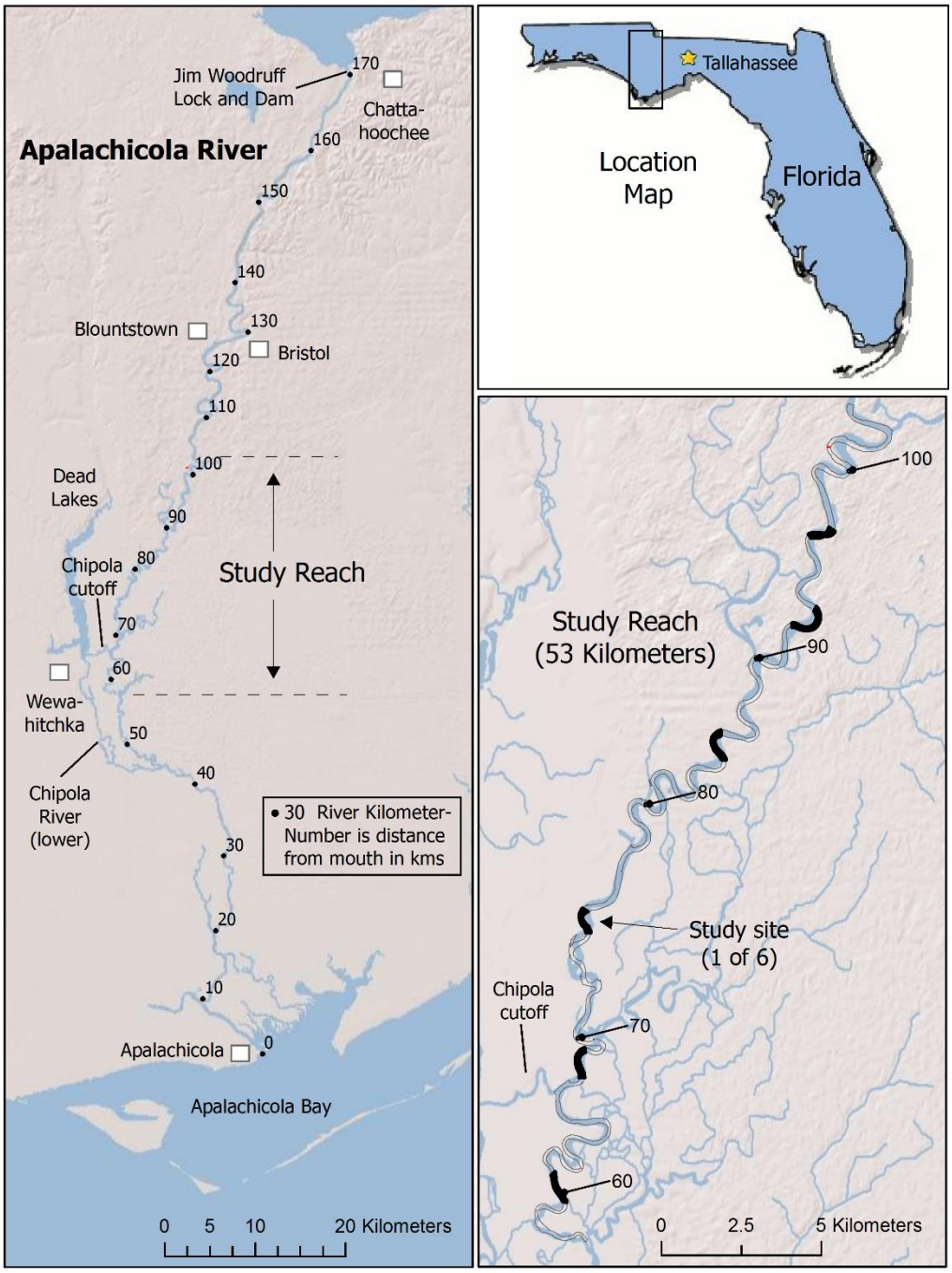

Figure 1. Study area.

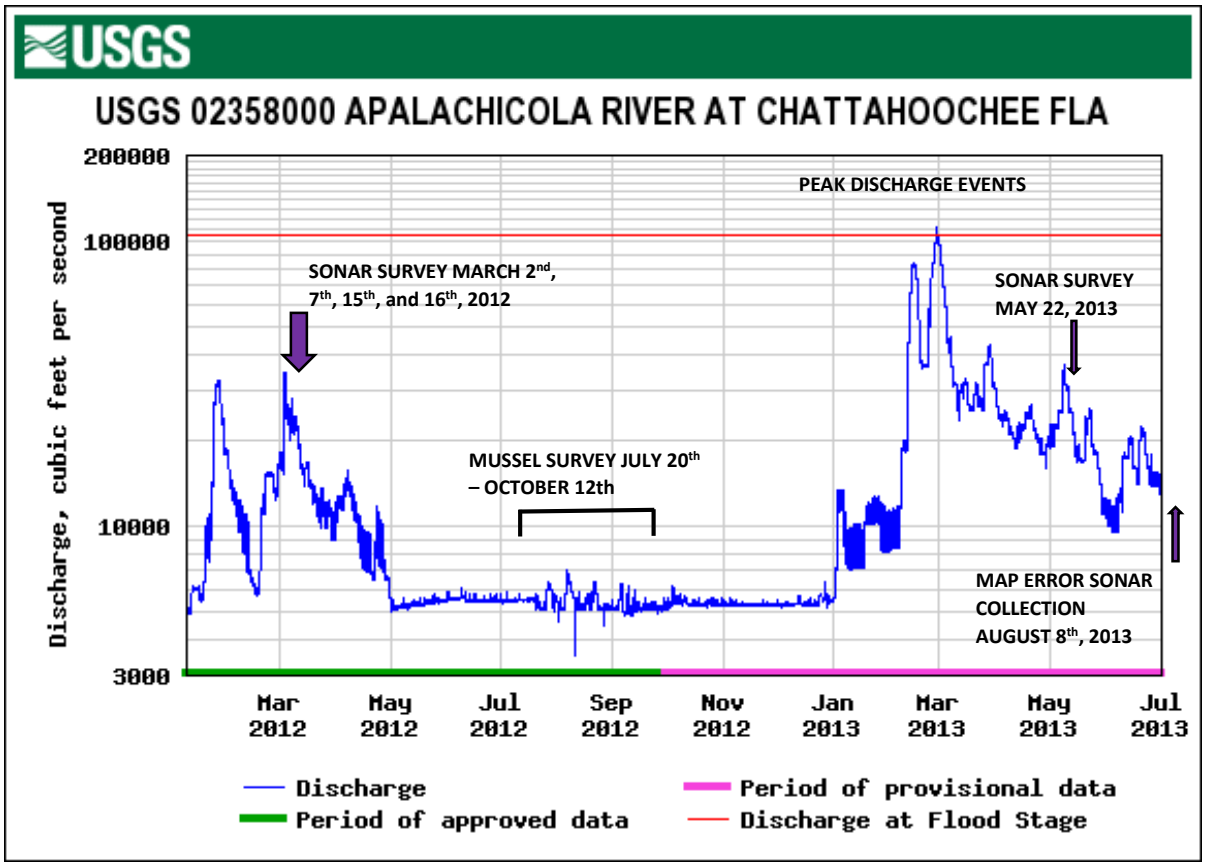

Figure 2. Dates of sonar data collection and associated discharges at the Jim Woodruff Lock and Dam USGS water gauge. Note the >100,000 cfs flood event occurring in March 2013, and the following sonar data collection used for the habitat change analysis.

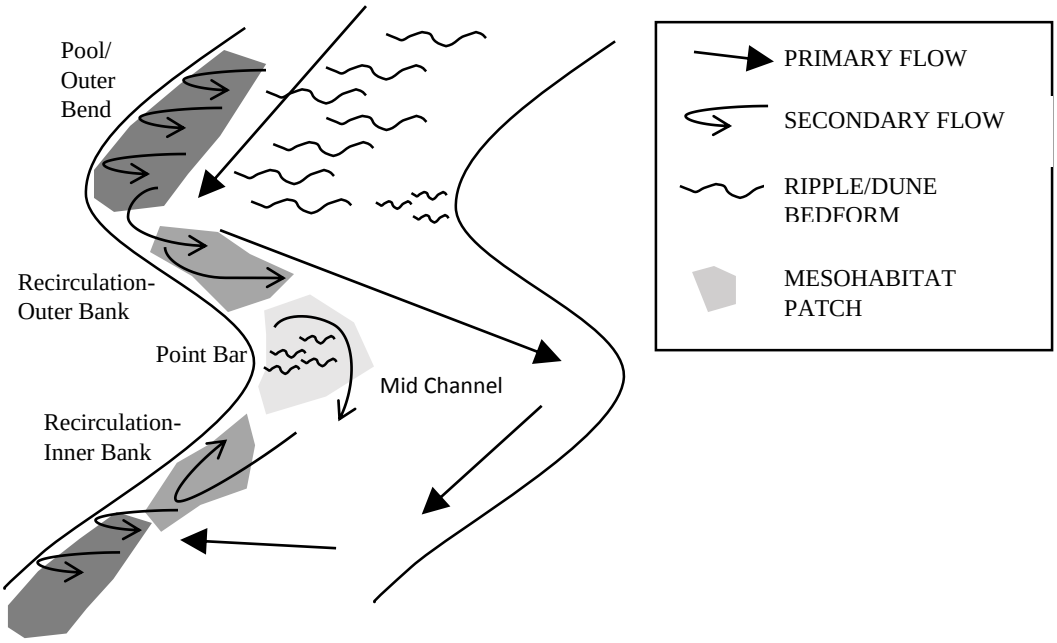

Figure 3. Conceptual illustration of the primary and secondary flow environments around a meander bend and associated habitat units used for this classification. Adapted from Garcia et al. 2012.

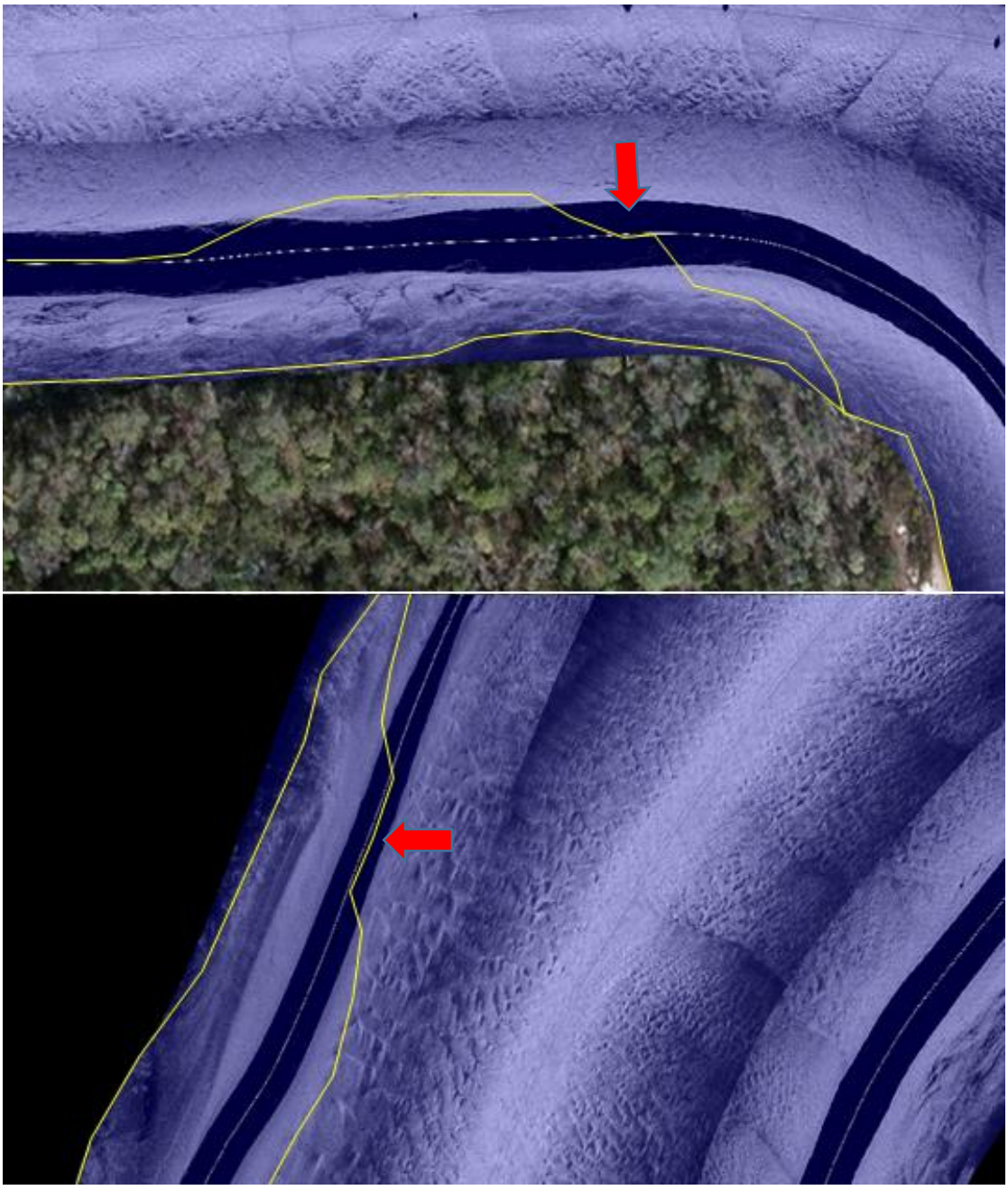

Figure 4 - Two examples of the standardized approach used to delineate boundaries, in this case the boundaries between recirculation zones and mid channel mesohabitats, when such boundaries crossed a region of the sonar image occupied by the water column (i.e., the dark band of pixels).

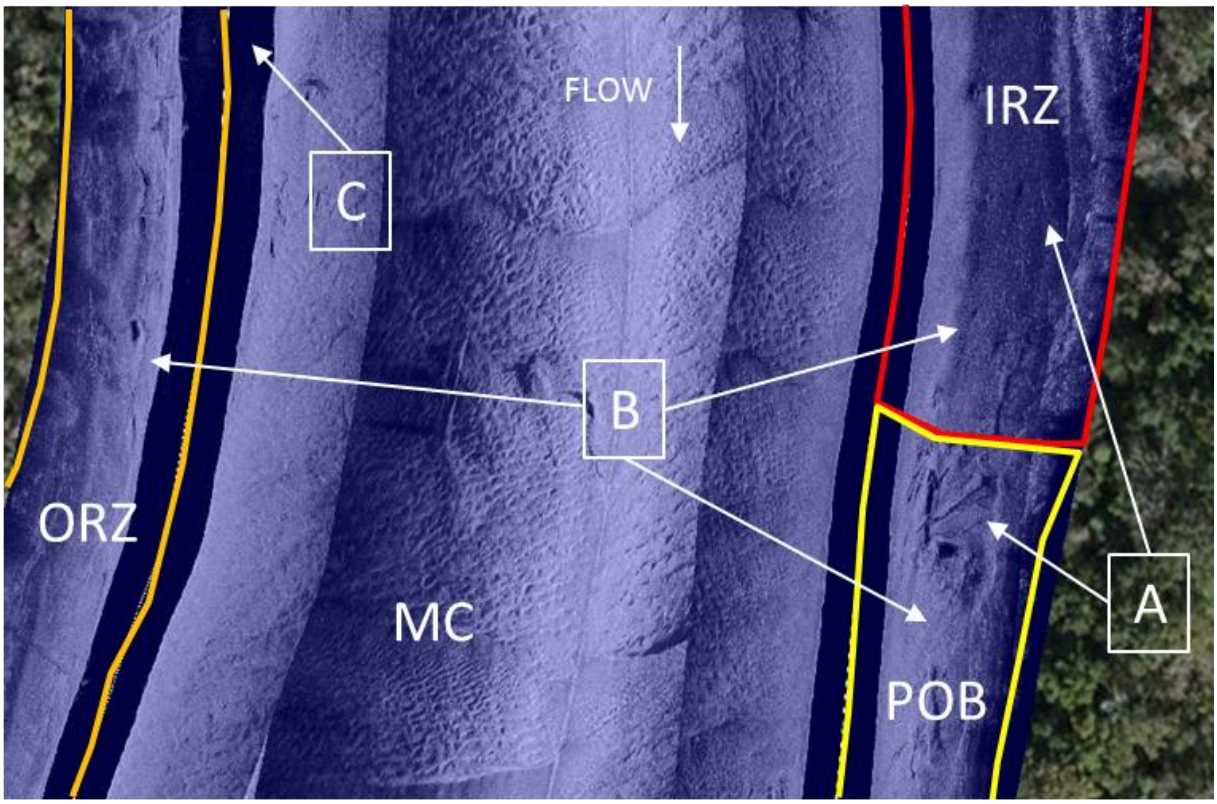

Figure 5-Detail of features used to distinguish the Inner and Outer Recirculation Zones from the Pool/Outer Bank and Mid-Channel habitats during mapping. A.) Using the dark tonal shift and appearance of large woody debris to delineated the IRZ from the POB. B.) Using the bedform variation from sand duned and rippled to smooth bedform to delineate the POB, IRZ, ORZ from the Mid-Channel. Bedform patterns inspected at a much finer map-scale during mapping (~1:300) than shown in this figure. C.) Dark band of pixels representing water depth. In this example, the boat passed directly over the smooth and duned bedform boundary during the time of collection, so the delineation proceeded across the center of the image.

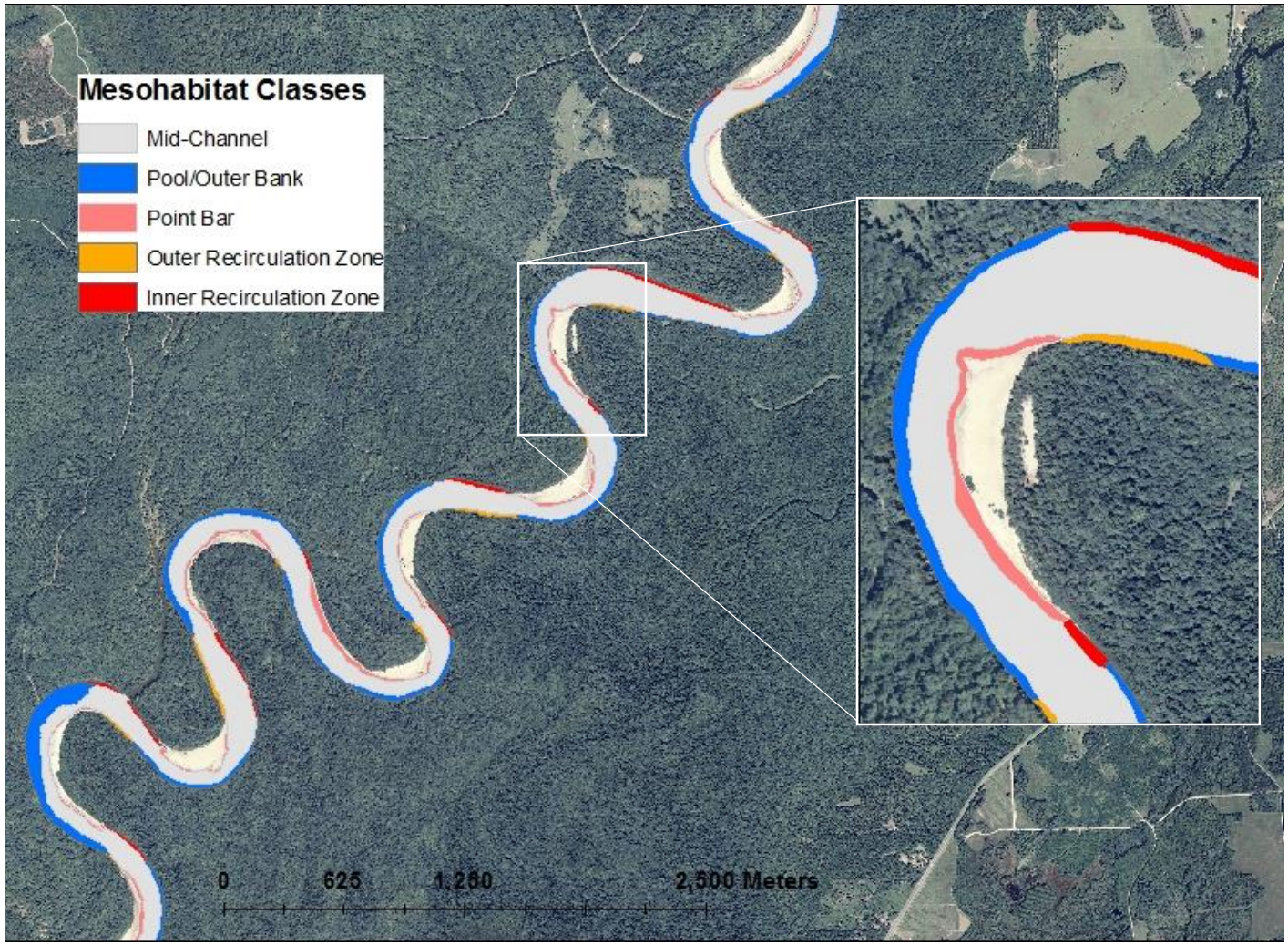

Figure 6 - A section of the completed mesohabitat classification map. Inset shows the consecutive, repeating nature of the mesohabitat classes around a typical meander bend.

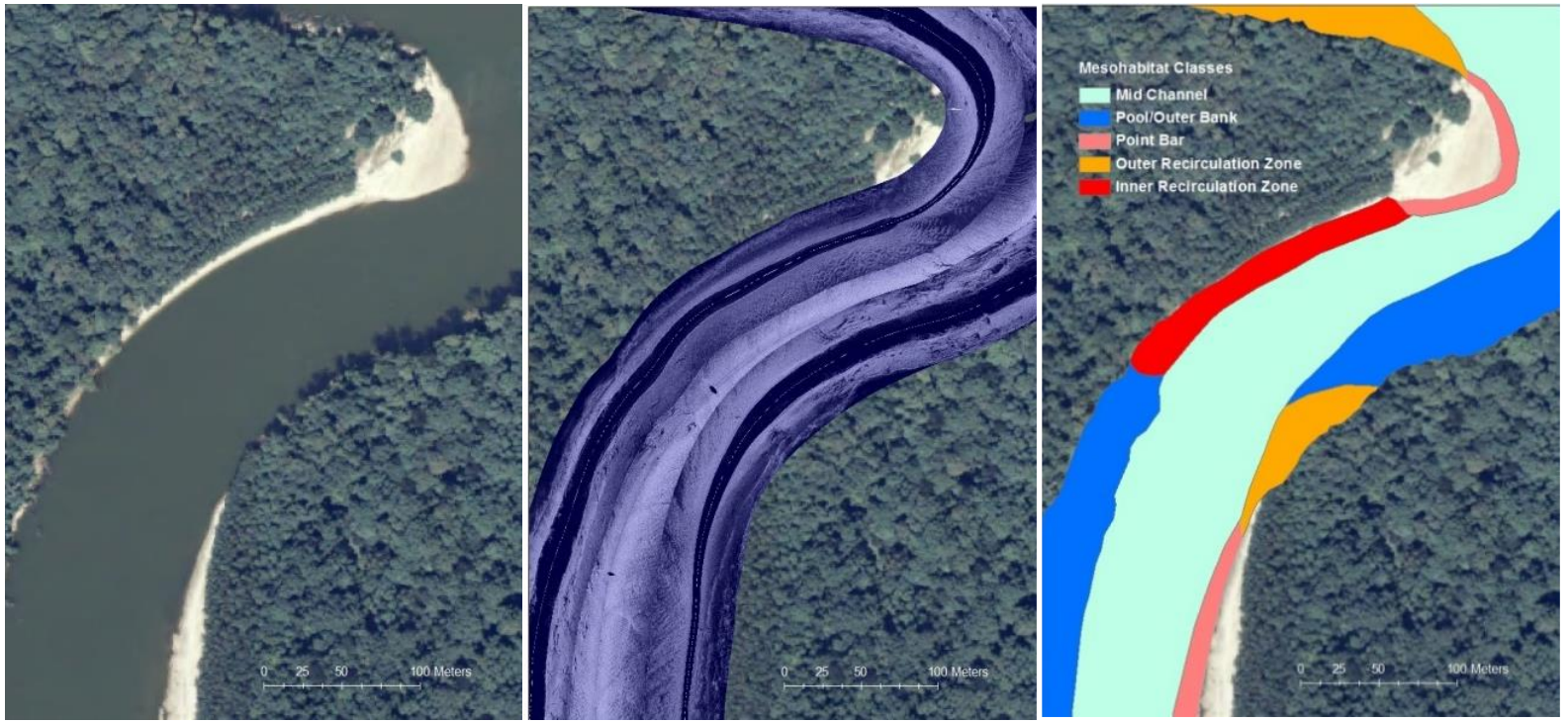

Figure 7- Panels illustrating the 2010 NAIP aerial imagery, sonar image map layers, and the classified mesohabitat map for a bend in the Apalachicola River.

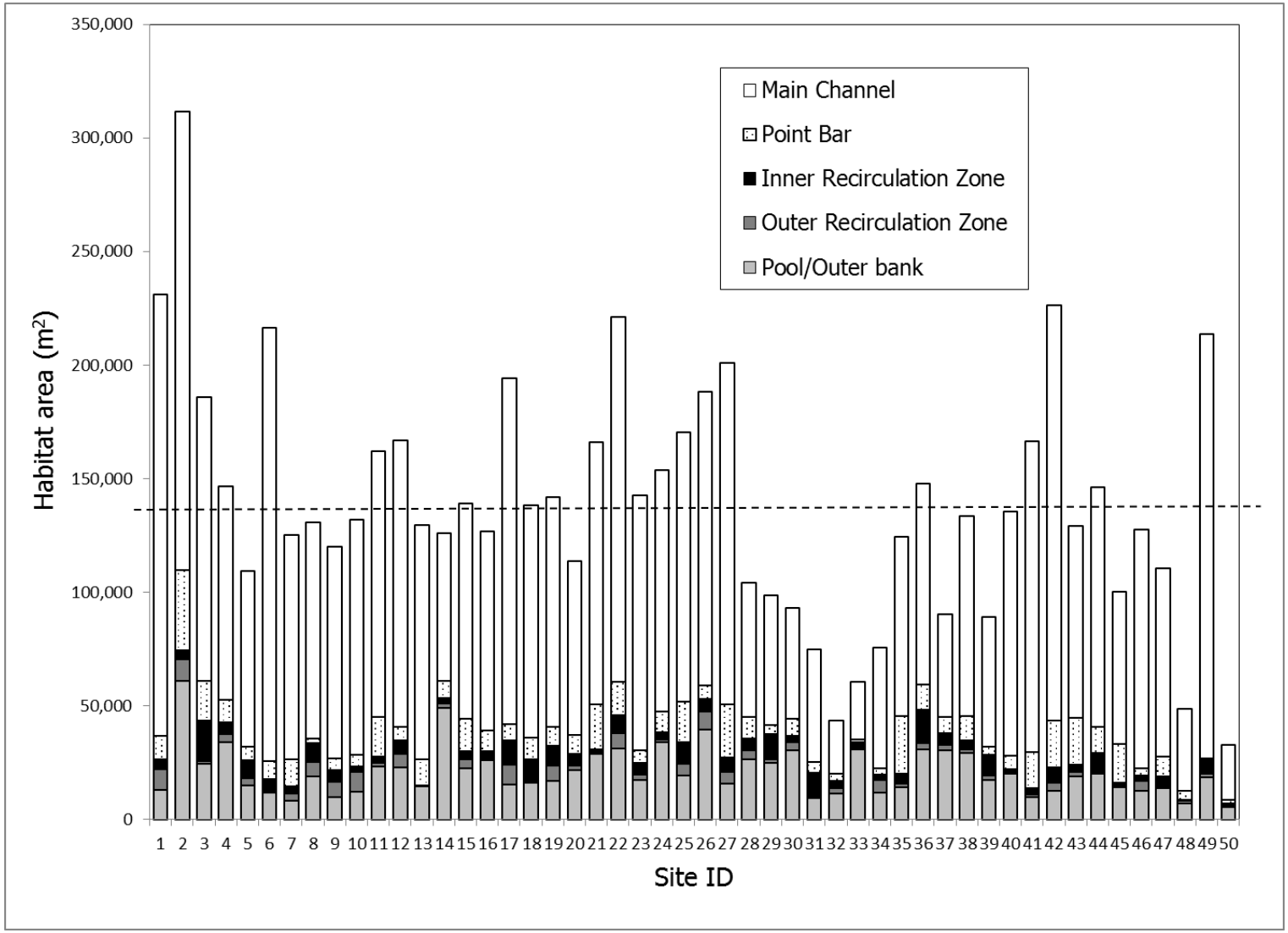

Figure 8. Breakdown of habitat area per site, where each site contains at least one of each mesohabitat type. Site ID number increases with distance downstream, so site 1 is the upstream extent of the study area and site 50 is the downstream extent. The dotted line represents the mean site area across all sites. Note sites 27 -34 hold consecutively smaller site areas.

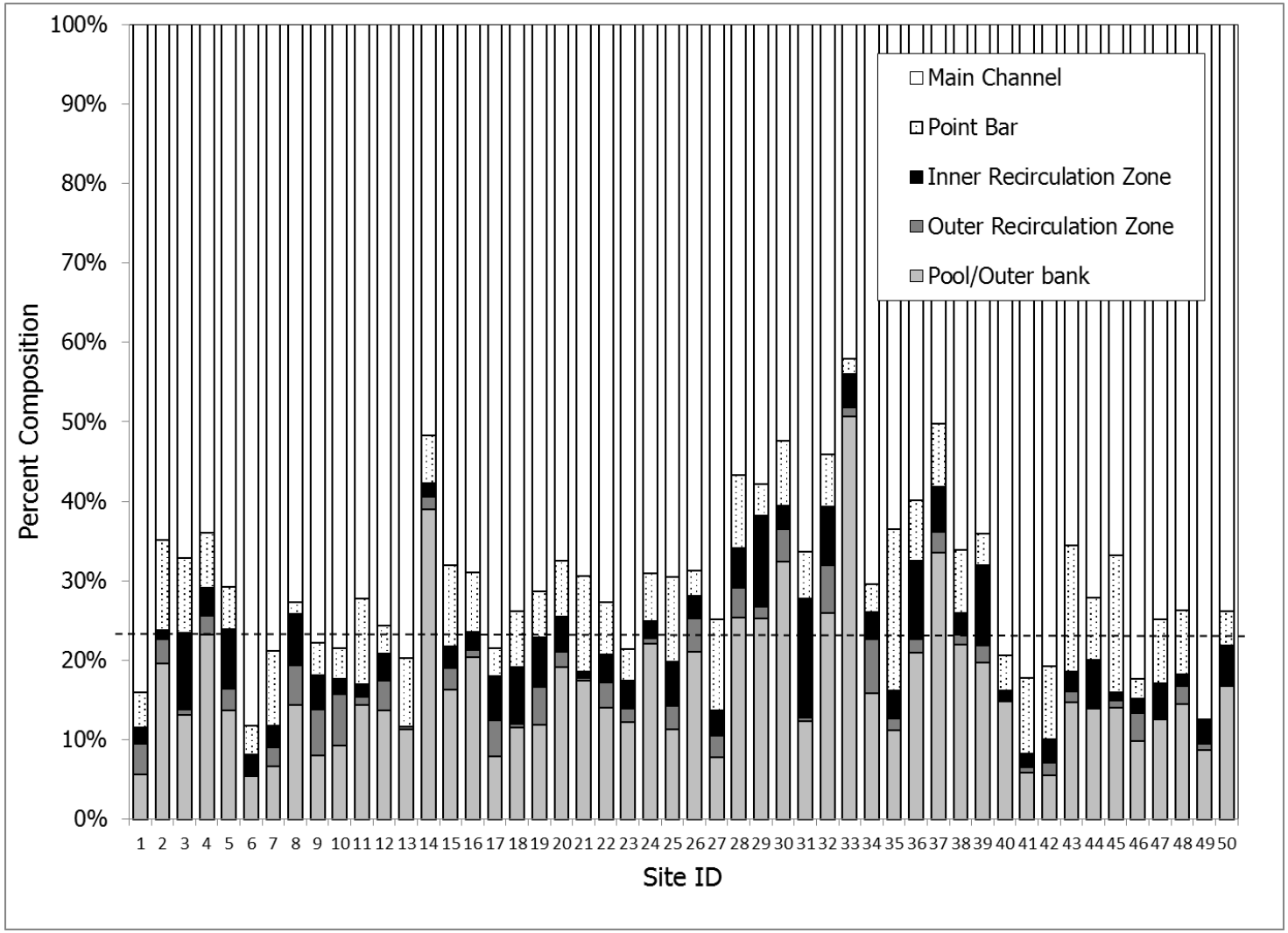

Figure 9. Proportion of area covered by each mesohabitat class per site. Note sites 27 to 39 show greater proportions of smooth bedform mesohabitats (IRZ, ORZ, POB) than all other sites.

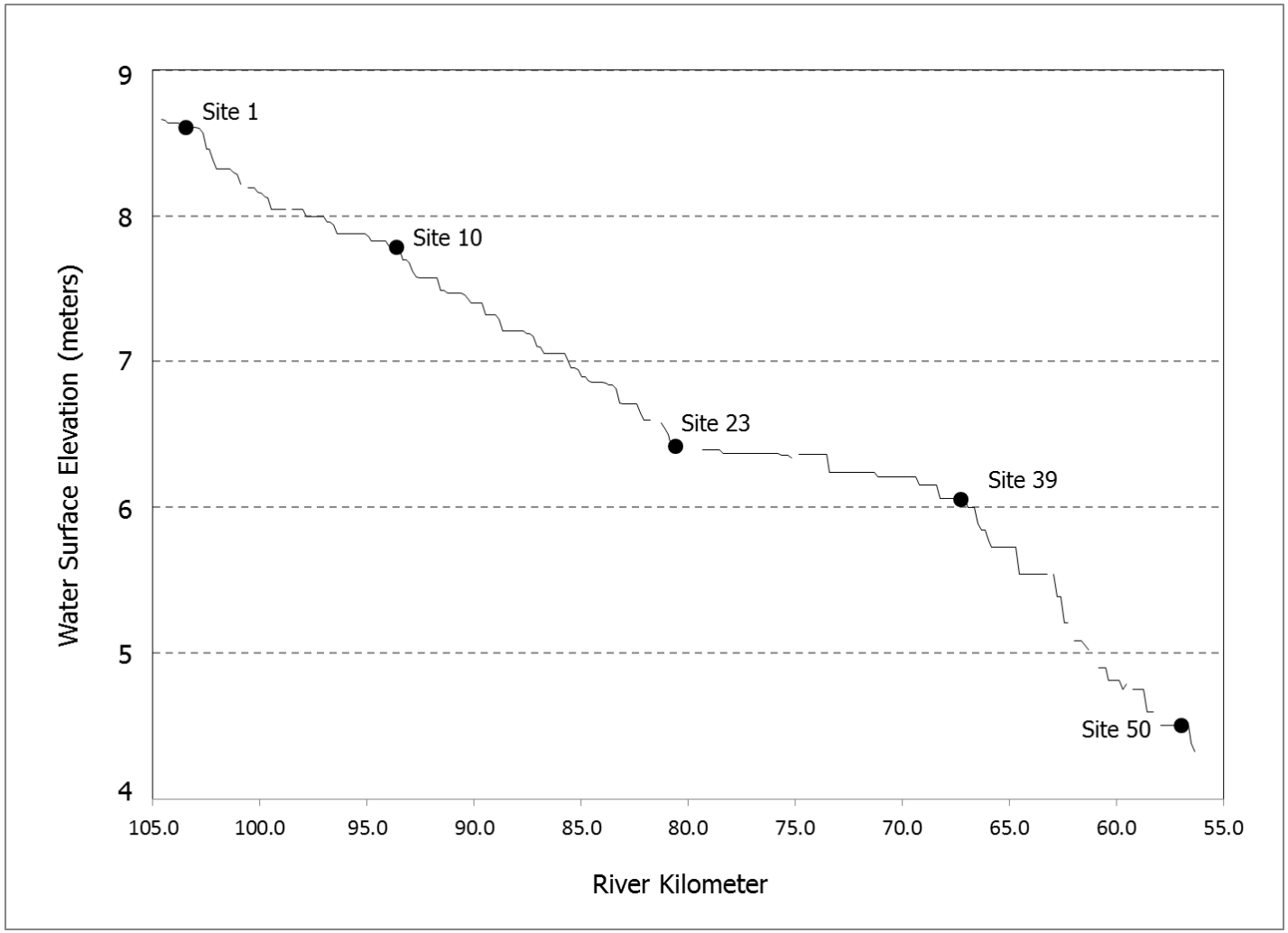

Figure 10. Gradient of the Apalachicola River across the study area. Note the change of gradient occurring from site 23 to 39.

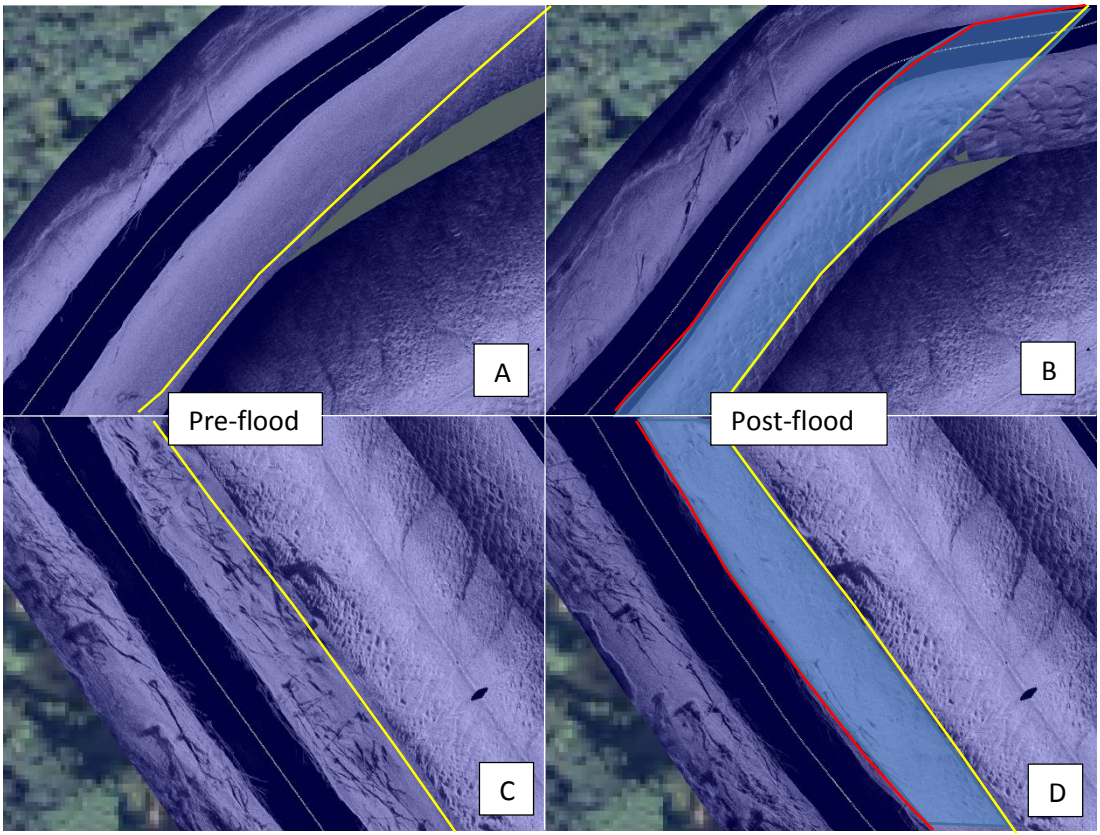

Figure 11. Example of sand dune and ripple bedform encroachment into smooth bedform habitats. Smooth bedforms in Recirculating-Inner Bank (A) and Pool/Outer Bank (C) experienced migration of sand ripples and dunes (B) and covering of large aggregations of woody debris (D). The yellow line represents the outer boundary of the smooth bedforms before the flood as they would be digitized in ArcGIS, while the red line indicates the boundary digitized after the flood. The area quantified as a decrease in habitat is the shaded portion in between the two boundaries, as analyzed using the raster calculator tool in ArcGIS. In A and B note the bedform and image tone remains consistent before and after the flood event, and in C and D, note the persistence of the large woody debris aggregations close to the bank.

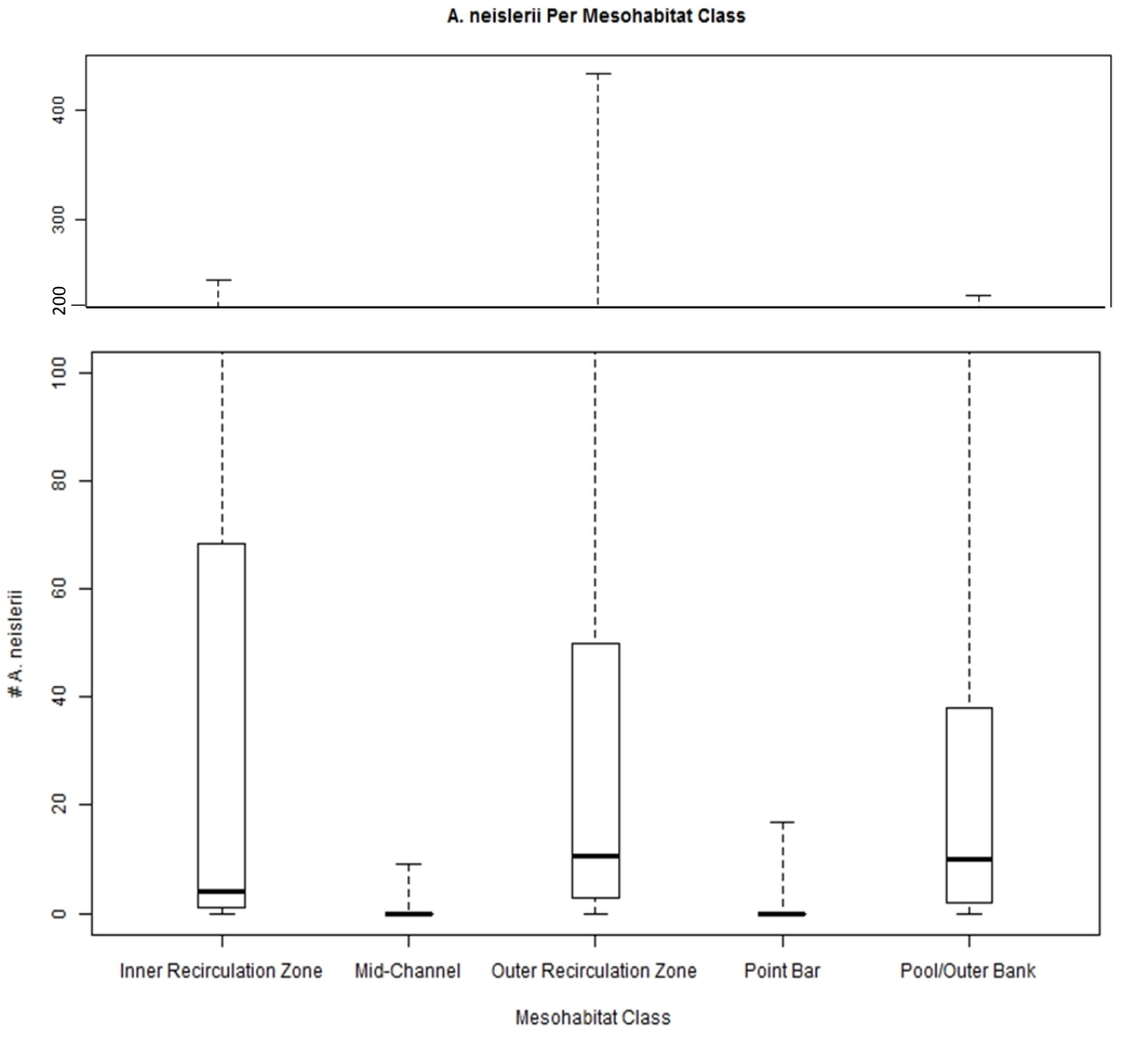

Figure 12. *A. neislerii* counts within each mesohabitat class. Boxes represent inner quartiles, and the solid horizontal black lines represent the median count. Dotted dashed lines represent the entire range of counts observed. Counts can be converted to density by dividing by the sampling area (10 m^2).

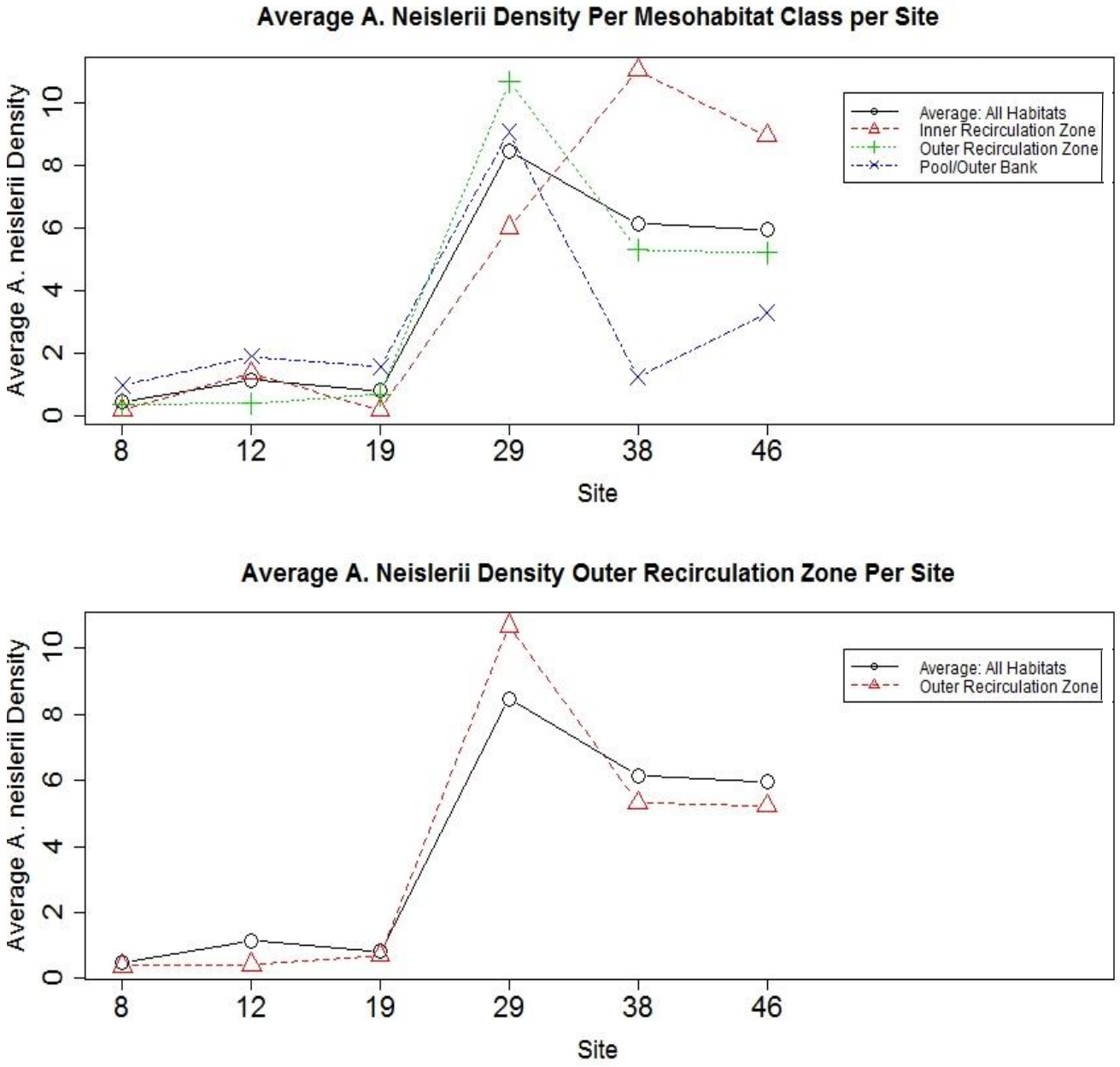

Figure 13. Trends in mean *A. neislerii* density between all mesohabitat classes (upper panel) and the Outer Recirculation Zone mesohabitat (lower panel) compared to average mean density across all mesohabitat classes for each sampling site. Sampling site number increases consecutively downstream. Note the large increase in average *A. neislerii* density at site 29 (river kilometer 75), and the congruency between average *A. neislerii* in the Outer Recirculation Zone mesohabitat class and average *A. neislerii* density across all samples.

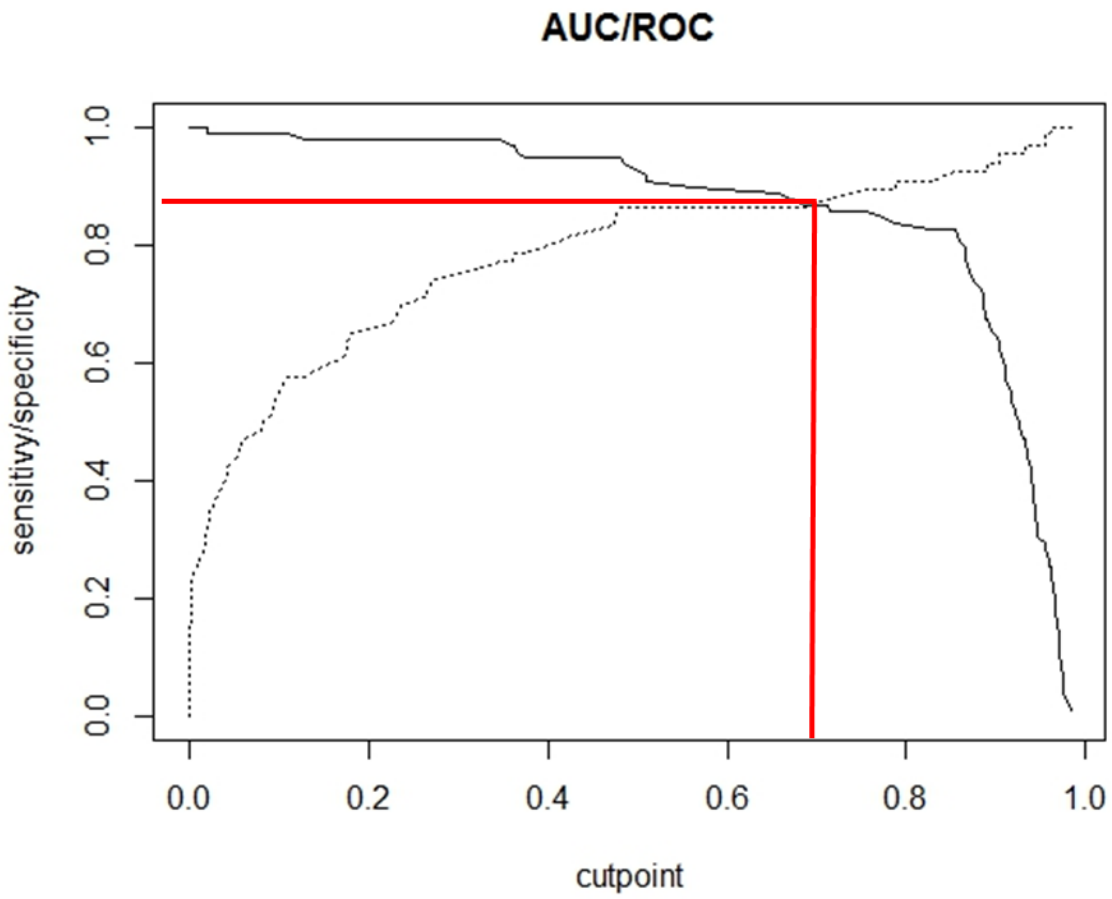

Figure 14. Plot of sensitivity versus specificity of the top ranking presence/absence logistic model. The plot revealed an optimal prediction probability to fall at 0.7 (vertical red line on the x-axis), and the AUC was found to equal 0.939 (horizontal red line on the y-axis).

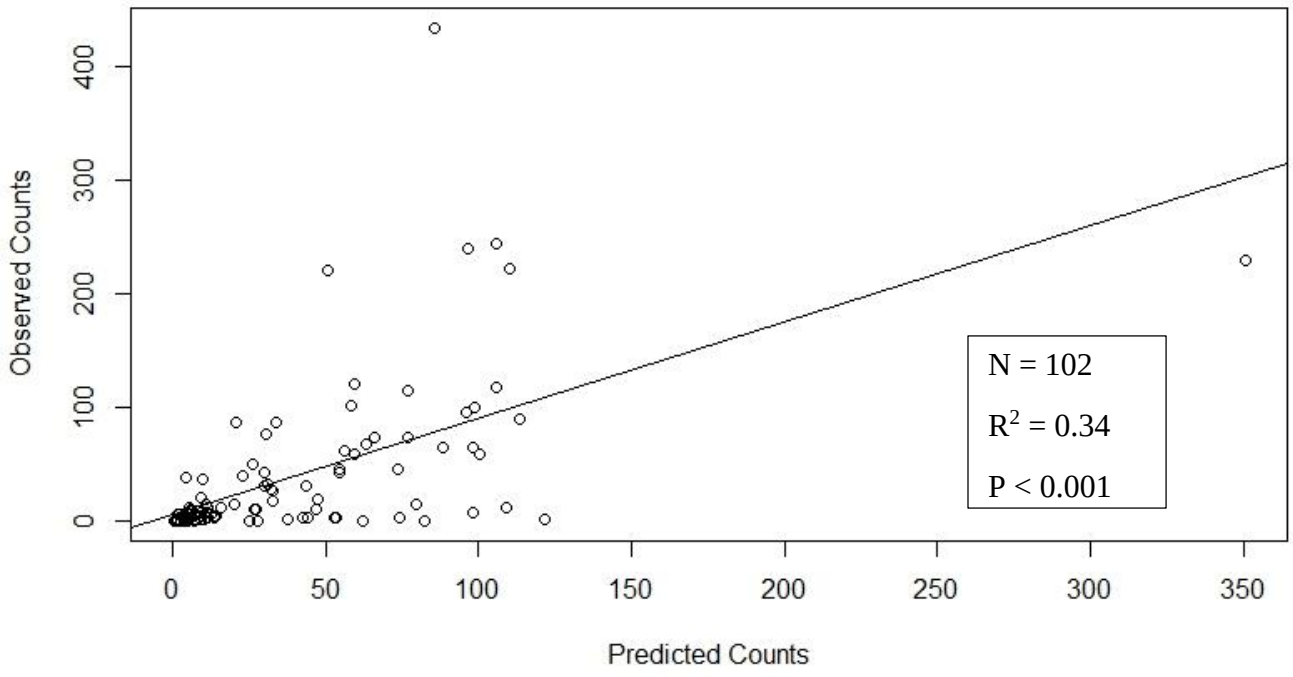

Figure 15. Observed *A. neislerii* counts from the survey vs. predicted counts from the top AIC_c ranked negative binomial generalized linear count model. Correlation coefficient (R^2) between points was found to equal 0.34, and the slope of the regression line (solid line) was found to equal 0.85.

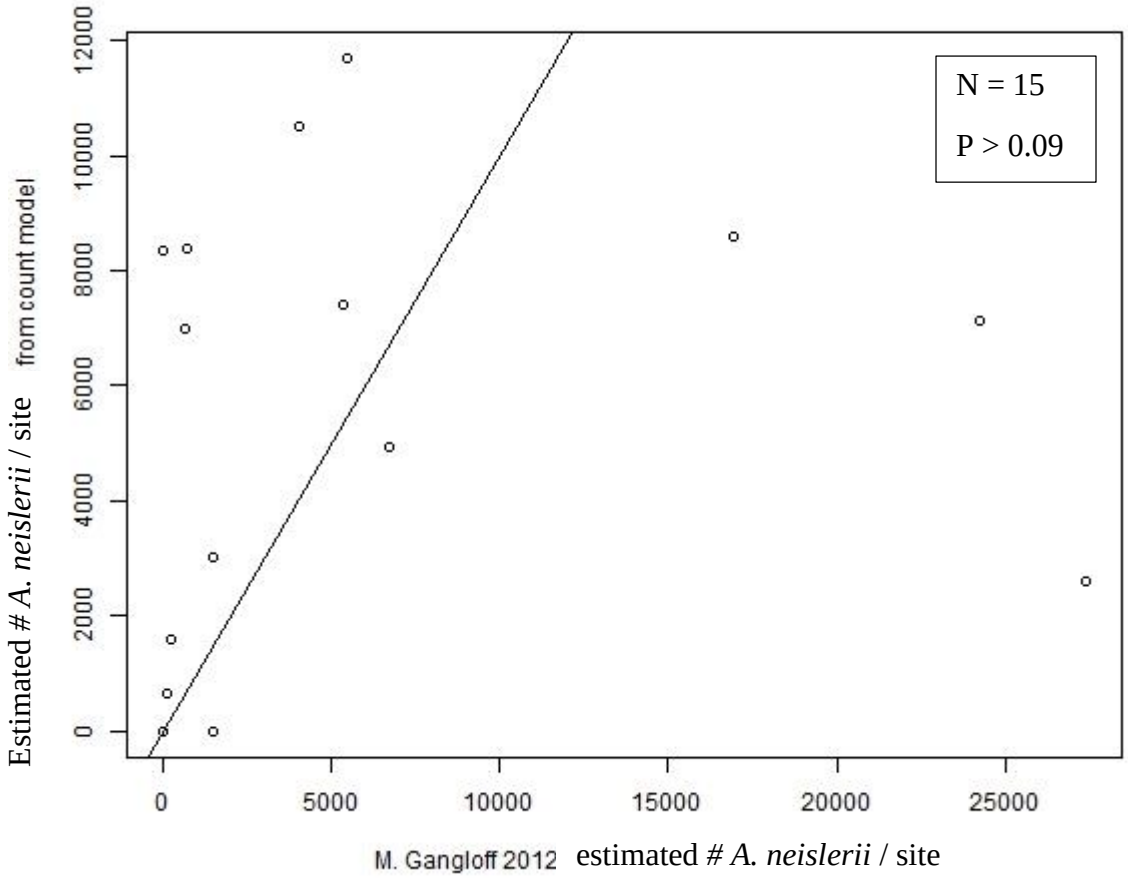

Figure 16. Site level comparisons of *A.* neislerii estimates between M. Gangloff's study in 2012 and the count model predictions estimated from within equal areas sampled by M. Gangloff in 2008, 2010, and 2011. $R^2 = 0.02$, and the slope of the regression line is equal to 1.12. Solid line represents a one to one relationship between *A. neislerii* count estimates from this study and Gangloff (2012).

Figure 17. Example of differences in sampling site area between M. Gangloff's 2012 study and the habitat extent identified with side scan sonar mapping of submerged bedform features. Polygons in each study represent habitat patches occurring at the meso-scale resolution of study.

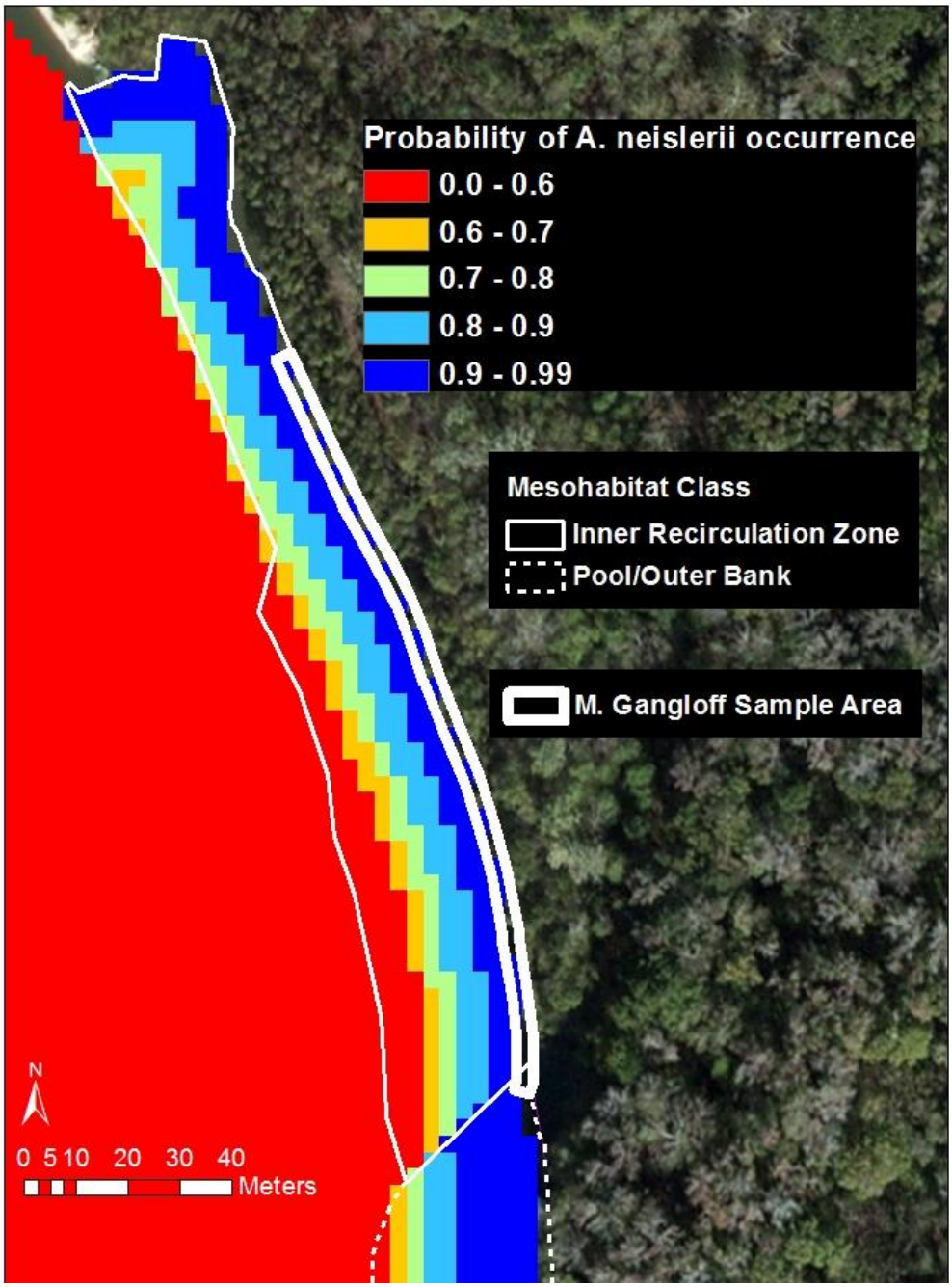

Figure 18. Geospatial species distribution model of presence/absence probabilities for *A. neislerii*. Probabilities of ≥0.7 were associated with the presence of at least 1 *A. neislerii* in a 10 m2 cell. Of note, the outer edge of the downstream portion of this Inner Recirculation Zone mesohabitat was predicted to have a low probability of *A. neislerii* occurrence. Gangloff's sampling area at this site represented a small fraction of the total mesohabitat area, but was located in an area of the highest predicted probability of *A. neislerii* occurrence.

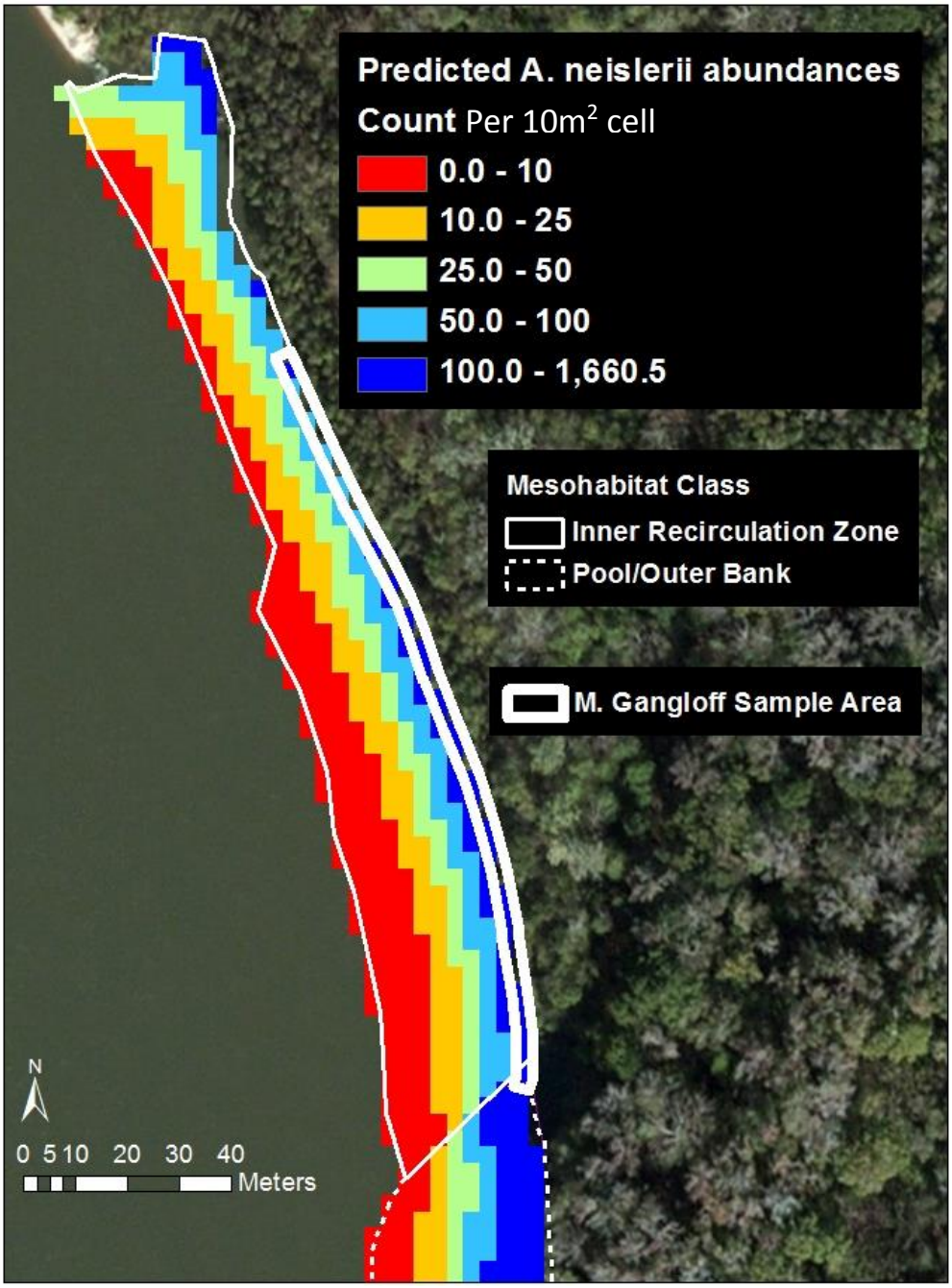

Figure 19. Geospatial species distribution model of abundance. Note area of M. Gangloff's sample site to be restricted to areas predicted to have the highest abundance. The total estimated abundance within the Inner Recirculation Zone mesohabitat shown here was 20901.3 mussels. Gangloff (2012) estimated that 5358.7 mussels inhabited the portion of this mesohabitat defined as the M. Gangloff sample area

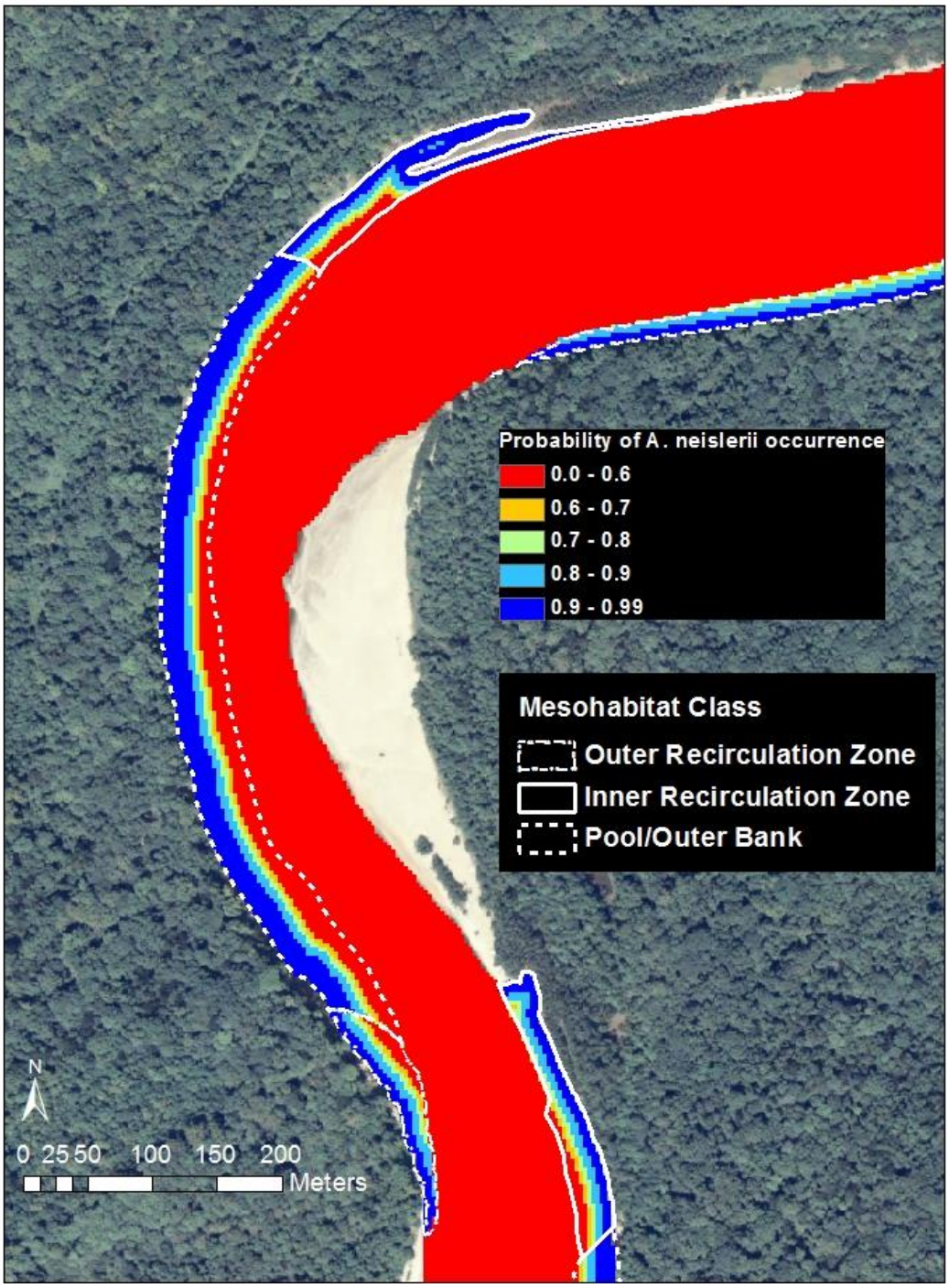

Figure 20. Site-level view of predicted probabilities of *A. neislerii* occurrence

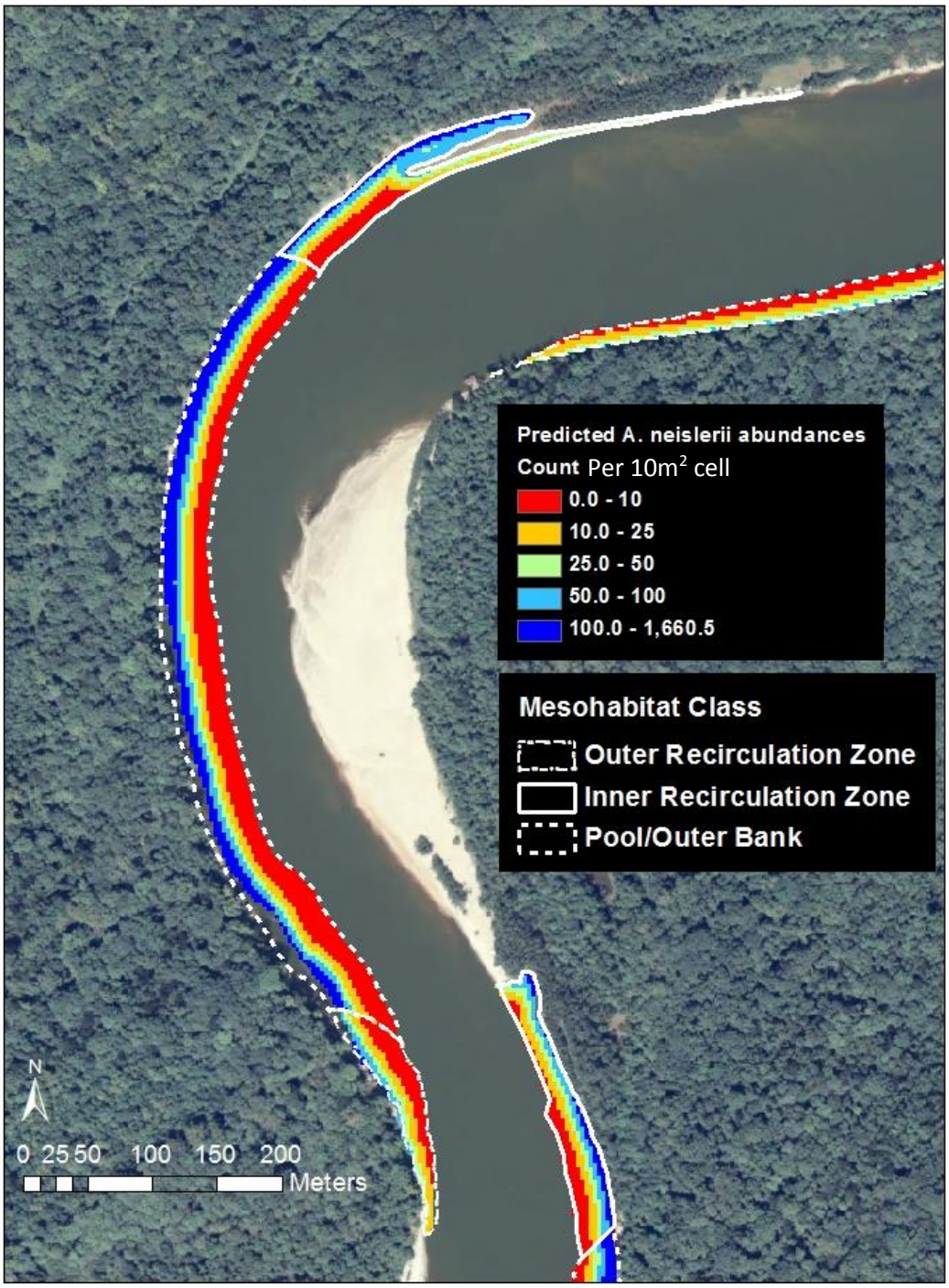

Figure 21. Site-level view of predicted *A. neislerii* abundance

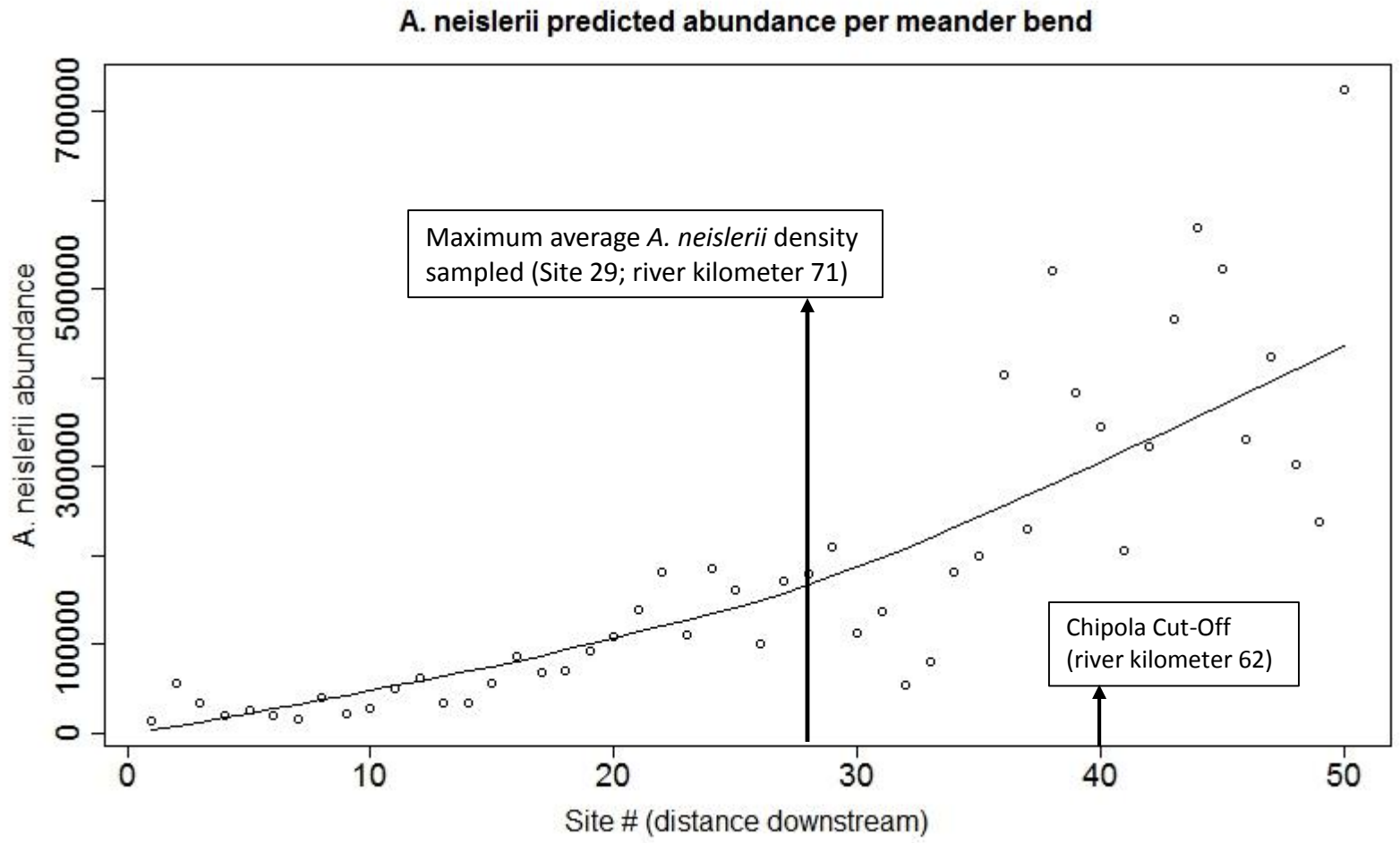

Figure 23. Trends in predicted number of *A. neislerii* per site. Sites correspond to the length of a single meander bend that contains at least one of each mesohabitat class for a total of 50 consecutive sites occurring from the upstream to downstream extent of the study area

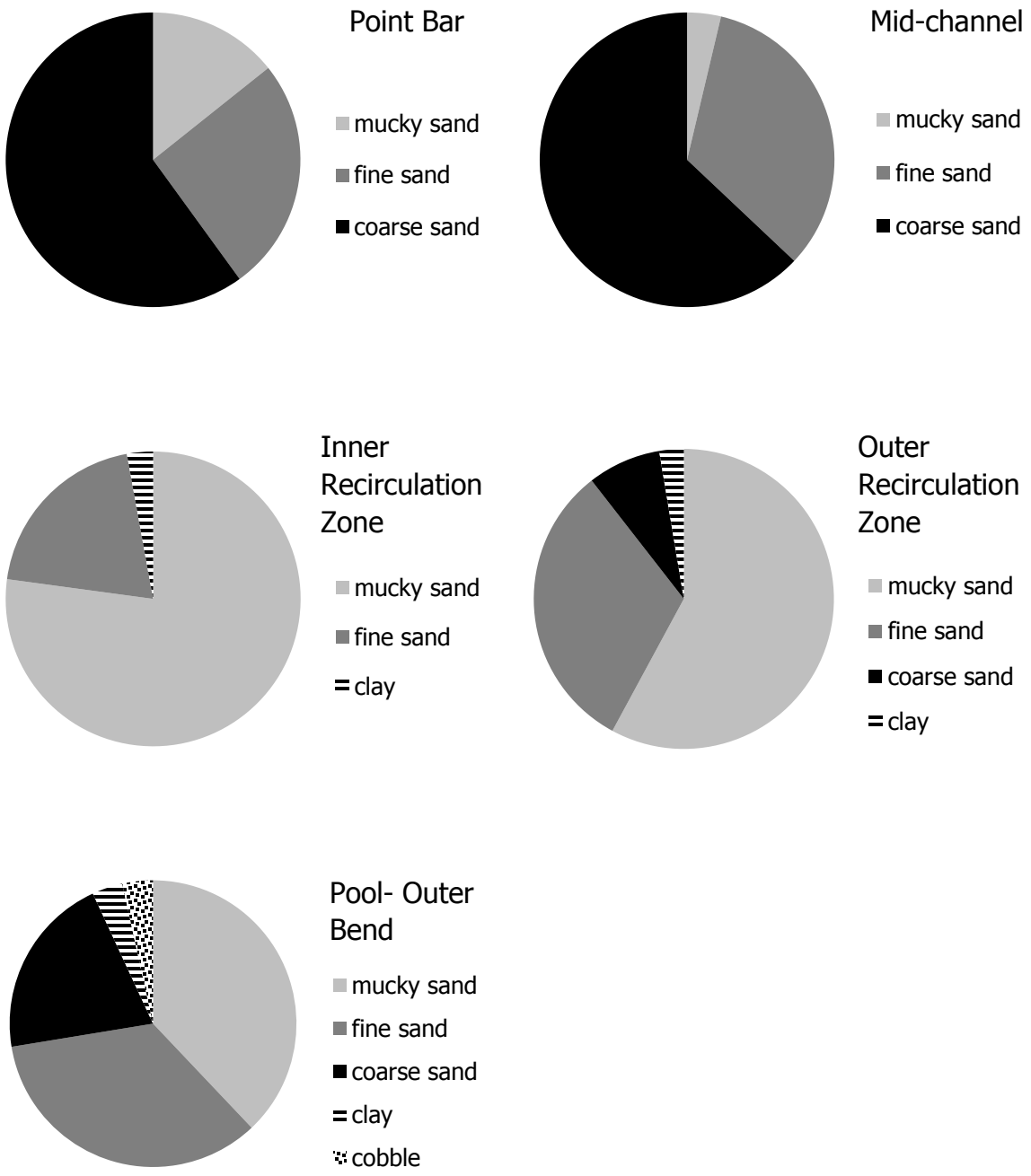

Figure 22. Composition of predominate substrate type of each sampling point per mesohabitat class. Mucky Sand = Combination of silt and finest sand particles.

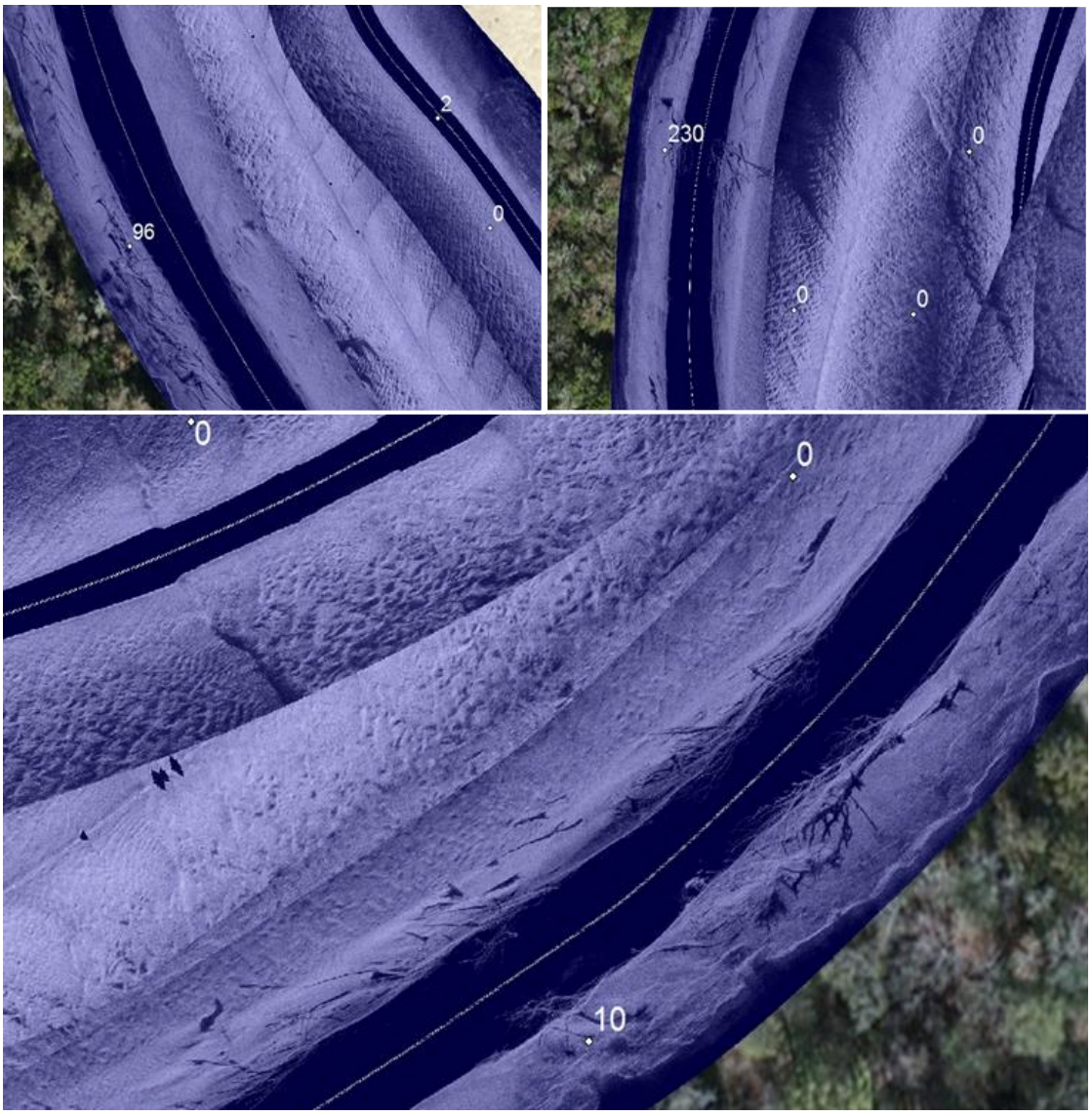

Figure 24. Associations between large aggregations of woody debris and counts of *A. neislerii*. Note the adjacent samples inside the sand ripples/dunes bedforms containing 0, while the samples located next to large woody debris structures contain 10, 96, and 230 *A. neislerii*.